

# Essential role of $\gamma$ -clade RNA-dependent RNA polymerases in rice development and yield-related traits is linked to their atypical polymerase activities regulating specific genomic regions

Vikram Jha<sup>1,2</sup> , Anushree Narjala<sup>1,3</sup> , Debjani Basu<sup>1</sup>, Sujith T. N.<sup>1,4</sup> , Kannan Pachamuthu<sup>1,5</sup>, Swetha Chenna<sup>1,3</sup> , Ashwin Nair<sup>1,3</sup>  and Padubidri V. Shivaprasad<sup>1</sup> 

<sup>1</sup>National Centre for Biological Sciences, GKVK Campus, Bangalore 560065, India; <sup>2</sup>BIOSS Centre for Biological Signaling Studies, Faculty of Biology, Albert-Ludwigs-Universität Freiburg, Freiburg im Breisgau 79104, Germany; <sup>3</sup>SASTRA University, Thirumalaisamudram, Thanjavur 613401, India; <sup>4</sup>University of Trans-Disciplinary Health Sciences and Technology, Bengaluru 560064, India; <sup>5</sup>Institut Jean-Pierre Bourgin, INRAE, AgroParisTech, Université Paris-Saclay, Versailles 78000, France

Author for correspondence:  
Padubidri V. Shivaprasad  
Email: shivaprasad@ncbs.res.in

Received: 27 April 2021  
Accepted: 14 August 2021

New Phytologist (2021) 232: 1674–1691  
doi: 10.1111/nph.17700

**Key words:** dsRNA, gene silencing, microRNAs, plant development, rice, RNA-dependent RNA polymerase, small RNAs.

## Summary

- RNA-dependent RNA polymerases (RDR) generate double-stranded (ds)RNA triggers for RNA silencing across eukaryotes. Among the three clades,  $\alpha$ -clade and  $\beta$ -clade members are key components of RNA silencing and mediators of stress responses across eukaryotes. However,  $\gamma$ -clade members are unusual in that they are represented in phylogenetically distant plants and fungi, and their functions are unknown.
- Using genetic, bioinformatic and biochemical methods, we show that  $\gamma$ -clade RDRs from *Oryza sativa* L. are involved in plant development as well as regulation of expression of coding and noncoding RNAs.
- Overexpression of  $\gamma$ -clade RDRs in transgenic rice and tobacco plants resulted in robust growth phenotype, whereas their silencing in rice displayed strong inhibition of growth. Small (s)RNA and RNA-seq analysis of OsRDR3 mis-expression lines suggested that it is specifically involved in the regulation of repeat-rich regions in the genome. Biochemical analysis confirmed that OsRDR3 has robust polymerase activities on both single stranded (ss)RNA and ssDNA templates similar to the activities reported for  $\alpha$ -clade RDRs such as AtRDR6.
- Our results provide the first evidence of the importance of  $\gamma$ -clade RDRs in plant development, their atypical biochemical activities and their contribution to the regulation of gene expression.

## Introduction

RNA silencing is a regulatory mechanism that employs small (s) RNAs and associated effector proteins to induce silencing at transcriptional or post-transcriptional levels across eukaryotes (Baulcombe, 2004). In plants, RNA silencing is mediated by 21–24-nt long sRNAs. Initiation of gene silencing requires the generation of double-stranded (ds)RNA, that can be generated either by bi-directional transcription of DNA, self-complementary RNA fold-backs, or through the action of specialised proteins called RNA-dependent RNA polymerases (RDRs) (Baulcombe, 2004; Matzke & Birchler, 2005). These dsRNA precursors are processed in a stepwise manner by Dicer-like (DCL) proteins into sRNAs. sRNAs are recognised by Argonaute (AGO) proteins to target RNAs complementary to the sRNA (Voinnet, 2008). The activity of this complex may include RNA cleavage or translational inhibition of the target mRNA, or methylation of specific DNA sequences (Brodersen *et al.*, 2008; Wu *et al.*, 2010).

The triggers for RNA silencing are dsRNAs. Among plants and worms, completely complementary dsRNA substrates are mostly generated by RDRs. Based on sequence similarity, RDRs have been divided into  $\alpha$ ,  $\beta$  and  $\gamma$ -clades. A family of RDRs that are conserved only among fungi and few animals are classified into  $\beta$ -clade and they seem to have roles in antiviral silencing (Zhang *et al.*, 2014). There are six members of RDRs in model plant *Arabidopsis thaliana* (three each in  $\alpha$ - and  $\gamma$ -clades, respectively), while their numbers are slightly fewer in larger genomes such as in *rice*, where there are five RDRs, three from the  $\alpha$ -clade and two that belong to the  $\gamma$ -clade (Wassenegger & Krczal, 2006; Willmann *et al.*, 2011).

Members of  $\alpha$ -clade RDR are involved in RNA silencing and related pathways among plants, fungi and worms. For example, AtRDR1 is mainly involved in viral RNA silencing, by converting viral single-stranded (ss)RNAs into dsRNA forms that are then cleaved by DCL4 into 21-nt sRNAs (Xie *et al.*, 2001; Bouché *et al.*, 2006; Diaz-Pendon *et al.*, 2007; Wang *et al.*, 2010;

Lee *et al.*, 2016). Mutants of AtRDR1 are phenotypically normal. RDR1 mostly provides defence against viruses and, in agreement with this, most RDR1 mutants are hypersusceptible to viral infections (Yang *et al.*, 2004). Surprisingly, RDR1 is also involved in resistance against herbivory in *Nicotiana attenuata* (Pandey & Baldwin, 2007). In addition, it has been shown that OsRDR1 is involved in DNA repair by helping in the production of qiRNAs (QDE-2 interacting sRNA) from aberrant RNAs (Chen *et al.*, 2013). Another member of the  $\alpha$ -clade, RDR2, is a nuclear protein involved in the production of 24-nt sRNAs by converting transcripts of plant-specific polymerase IV (PolIV), which are subsequently cleaved by DCL3. This transcriptional silencing pathway is involved in the regulation of repeats and transposons, involving DNA-methylation and histone modifications (Xie *et al.*, 2004; Lu *et al.*, 2006; Matzke *et al.*, 2009; Bologna & Voinnet, 2014; Blevins *et al.*, 2015; Singh *et al.*, 2019). Similar to RDR1, RDR2 mutants are phenotypically normal in *A. thaliana*. RDR6, conversely, is involved in the production of 21-nt secondary siRNAs that are hallmarks of post-transcriptional gene silencing (PTGS), such as *trans*-acting si(tasi)RNAs, virus-induced silencing, and transgene silencing (Dalmay *et al.*, 2000; Mourrain *et al.*, 2000; Peragine *et al.*, 2004; Vazquez *et al.*, 2004; Yoshikawa, 2005). Recent evidence also indicates that 21/22-nt siRNAs generated through the action of RDR6 participated in transcriptional gene silencing (Nuthikattu *et al.*, 2013; Cuerda-Gil & Slotkin, 2016). RDR6 silenced lines in *A. thaliana* show downward curling of rosette leaves (Vazquez *et al.*, 2004), whereas rice RDR6 mutant was normal (Hong *et al.*, 2015). Overexpression of RDR6 in Arabidopsis had no effect on growth and development of the plant (Curaba & Chen, 2008). Although DCL4 and RDR6 regulate hundreds of sRNA loci in the genome, mutations in them are associated with differential production of ta-siRNAs and mis-regulation of few ARFs loci to induce a leaf curling phenotype (Peragine *et al.*, 2004; Vazquez *et al.*, 2004; Allen *et al.*, 2005; Yoshikawa, 2005; Adenot *et al.*, 2006; Fahlgren *et al.*, 2006; Garcia *et al.*, 2006). It has been reported that *ty-1* and *ty-3* loci in tomato that share high sequence similarity to DFDGD (conserved catalytic motif in  $\gamma$ -clade RDRs) class of RDRs, are involved in resistance against DNA viruses (Verlaan *et al.*, 2013; Butterbach *et al.*, 2014). However, functions of  $\gamma$ -clade RDRs in plants are largely unknown. Expression analysis showed that AtRDR3, 4 and 5 members of  $\gamma$ -clade, express well in the apex of inflorescence (Willmann *et al.*, 2011), although these RDR members were never functionally characterised. Viral polymerases that use RNA as substrate for viral genome replication are also known as RNA-dependent RNA polymerases (RdRps), however they are shorter than eukaryotic RDRs, with huge sequence variations (Bruenn, 1991, 2003; Gorbalenya *et al.*, 2002).

Biochemical characterisation of a few eukaryotic RDRs has been undertaken, for example tomato RDR was able to catalyse RNA synthesis *in vitro* (Schiebel *et al.*, 1993a, 1998). RDR activity was routinely detected in the extracts of several plants (Astier-Manificier & Cornuet, 1971, 1978; Duda, 1979; Ikegami & Fraenkel-Conrat, 1979; Xie *et al.*, 2001; Tang, 2003). These experiments have indicated that RDRs have both primer-

dependent and independent activities, *in vivo* and *in vitro* (Schiebel *et al.*, 1993b; Tang, 2003; Curaba & Chen, 2008; Devvert *et al.*, 2015). Most of these RDRs are sequence and template independent (Curaba & Chen, 2008). For unknown reasons, the newly formed transcript remains hybridised to the parental strand (Curaba & Chen, 2008; Devvert *et al.*, 2015). All these functions are key differences that distinguish eukaryotic RDRs from viral RdRps that perform *de novo* synthesis, where the first nucleotide acts as a primer or in a primer-independent manner but requiring specific structure in the 3'-end of the templates (Honda *et al.*, 1986; Paul *et al.*, 1998; Kao *et al.*, 1999). Purified RDR named QDE1 from *Neurospora crassa*, had polymerase activity on both ssRNA and ssDNA substrates (Makeyev & Bamford, 2002; Liu *et al.*, 2010). QDE1 can also generate short ssRNA from ssRNA and circular ssDNA templates (Makeyev & Bamford, 2002; Liu *et al.*, 2010). QDE1, together with replication protein A and DNA helicase, produce dsRNA and aberrant RNA after DNA damage in *Neurospora* (Liu *et al.*, 2010).

Reports on the function of  $\gamma$ -clade RDRs are limited, although they are conserved across plants and fungi. Here we report the functional characterisation and biochemical activities of  $\gamma$ -clade RDRs named OsRDR3 and OsRDR4 from rice. We found that OsRDR3-overexpressing rice plants (OE) showed vigorous growth and increase in tiller number by contrast with RDR3 artificial miRNA (amiR) knockdown (KD) lines that have stunted growth and that did not survive beyond vegetative growth. RDR4 OE plants exhibited less intense vigorous growth phenotype when compared with OsRDR3 OE plants. However, OsRDR4 KD lines had stunted growth and severe defects in panicles resulting in poor seed setting. sRNA and RNA-seq analysis in OsRDR3 OE and KD lines identified hundreds of transposons and repeat-rich loci where RDR3 induced production of 21-nt and 24-nt sRNAs. Biochemically, OsRDR3 synthesised abundant new RNAs from both ssRNA and ssDNA templates. Our results indicated novel functions of  $\gamma$ -clade OsRDR3 in plant development and regulation of gene expression, likely to be through its polymerase activities.

## Materials and Methods

### Protein sequence alignment and phylogenetic tree construction

Plant RDR sequences were downloaded from UniProt and aligned in GENEIOUS 11.0.3 software (<https://www.geneious.com>). The phylogenetic tree was constructed using a neighbour-joining algorithm in MEGA 7.0 (Kumar *et al.*, 2018) with 100 bootstraps. The phylogenetic tree was fine tuned using the iTOL online server (Ciccarelli, 2006).

### Plasmid constructions

Full-length cDNA of OsRDR3 was amplified from *Oryza sativa* indica Pusa Basmati 1 (PB1) callus and cloned into the pGEM-T easy vector (Promega). For generating RDR3 OE lines of rice, RDR3 (coding sequence of 2499 bp; 832 aa) was cloned into the

pCambia1300 vector. RDR3 amiR construct was designed using WMD tool (<http://wmd2.weigelworld.org>). For generating GFP-RDR3 OE transgenic *Nicotiana tabacum*, RDR3 was cloned into modified the pCambia1300 vector containing an N-terminal mGFP tag. For translational fusion of RDR3 with maltose-binding protein (MBP), RDR3 was cloned into the modified pMAL-p5E vector (NEB, Ipswich, MA, USA) having an N-terminal MBP tag under the tac promoter. For creating mutation in the conserved catalytic domain, the MBP-RDR3 plasmid was amplified by RDR3\_MBP\_D-A mut\_fw and RDR3\_MBP\_D-A mut\_Rv primers (Supporting Information Table S1) to substitute the 693<sup>rd</sup> D to A, treated with *DpnI* (NEB) and transformed into *Escherichia coli* DH5 $\alpha$  competent cells. OsRDR4 was amplified from PB1 and cloned into the pGEM-T easy vector (Promega). For generating GFP-RDR4 OE lines of rice, RDR4 was cloned into the pCambia1300 vector by GIBSON assembly. The RDR4 amiR construct, where amiR was driven by the maize ubiquitin promoter was designed using the WMD tool (<http://wmd2.weigelworld.org>).

## Plant transformation

Rice transformation was performed as described earlier (Sridevi *et al.*, 2008). Tobacco was transformed using the leaf disc method as described previously (Shivaprasad *et al.*, 2006).

## sRNA library preparation, sequencing and analysis

sRNA sequencing libraries were prepared with the TruSeq sRNA Sample Preparation Guide (Illumina, San Diego, CA, USA) and sequenced on the Illumina NextSeq500 platform in two biological replicates. The sRNA-seq reads were adapter trimmed, filtered for invalid sequences and retained reads of length ranged between 20 and 25-nt using the UEA sRNA Workbench v.3 (Stocks *et al.*, 2012). Processed reads were aligned to the *O. sativa* japonica genome (IRGSP1) allowing one mismatch using BOWTIE (Langmead *et al.*, 2009). Library sizes were normalised by calculating reads per million (RPM) of 20 to 25-nt genome matched sRNAs. The abundance of known miRNAs (Table S2) was determined using miRProf (Stocks *et al.*, 2012). sRNAs mapping to different genomic features were determined using the annotation file from Ensembl plants and a repeat annotation file from TIGR. The sRNA sequences were submitted to GEO datasets (accession nos. GSE115056-OsRDR3 and GSE181778-OsRDR4). sRNA clusters across the genome were determined using SHORTSTACK v.3.8.5, with default parameters (Johnson *et al.*, 2016). EDGEr was used to identify differentially expressed sRNA with loci fold change cut-off of 1.5 and an FDR < 0.05.

## RNA sequencing and analysis

Paired-end (150  $\times$  2) RNA-seq reads were adapter trimmed using CUTADAPT (Martin, 2011) and aligned to the genome (IRGSP1) using HISAT2 (Kim *et al.*, 2019). Differential expression analysis was performed using CUFFDIFF (Trapnell *et al.*, 2011), and GO analysis was performed using AGRIGO v.2.

## Protein expression and purification from *E. coli*

MBP-RDR3 wild-type (WT) and mutant constructs were transformed into C41 (DE3) cells. Protein expression was induced in secondary culture at 0.6 OD, by 0.1 mM IPTG at 25°C for 10 h. Cells were pelleted down and resuspended in 20 ml of lysis buffer (50 mM Tris-HCl pH 7.6, 250 mM NaCl, 5% glycerol, 3 mM  $\beta$ -mercaptoethanol, 5 mM MgCl<sub>2</sub> and one tablet of EDTA-free protease inhibitor (Sigma-Aldrich)). Cells were lysed by sonication (65% amplitude, 10 s pulse on, 35 s pulse off for 10 min in ice) and centrifugation was performed at 30 900 *g* for 1 h at 4°C. The supernatant was passed through a 0.45- $\mu$ m syringe filter (Millex-HV). MBP beads (dextrin sepharose; GE Healthcare, Chicago, IL, USA) were first washed with eight column volumes (CV) of buffer A (50 mM Tris-HCl pH 7.6, 200 mM NaCl, 5% glycerol and 5 mM MgCl<sub>2</sub>) and the protein lysate was passed through the beads slowly. Beads were again washed with eight CV of buffer A, then eight CV of buffer B (50 mM Tris-HCl pH 7.6, 1 M NaCl, 5% glycerol and 5 mM MgCl<sub>2</sub>) and again with eight CV of buffer A. Finally, the protein was eluted in 6 ml of elution buffer (50 mM Tris-HCl pH 7.6, 200 mM NaCl, 5% glycerol, 5 mM MgCl<sub>2</sub> and 15 mM maltose). The eluted protein was concentrated using Amicon ultracentrifugal filters (50 kDa cut-off). The concentrated protein was further purified using a HiLoad Superdex 200 pg preparative size exclusion chromatography (SEC) column (GE Healthcare). The fraction containing the MBP-RDR3 protein (fraction 2–9) was pooled and again concentrated using Amicon ultracentrifugal filters (50 kDa cut-off).

## RNA and DNA templates

A 60-nt long ssRNA corresponding to the 853–912 region of e-GFP was purchased from IDT (Table S1). PAGE-purified 74-nt long ssDNA oligos were obtained from Bioserve (Hyderabad, India; Table S1).

## RDR activity assay

RNA-dependent RNA polymerase activity assays were performed as described previously (Makeyev & Bamford, 2002) with some modifications. Briefly, an assay was conducted in a 30  $\mu$ l reaction mixture containing 50 mM HEPES-KOH, 20 mM ammonium acetate, 1% polyethylene glycol (PEG) 8000 (w/v), 10 mM MgCl<sub>2</sub>, 0.1 mM EDTA, 0.25 mM each of ATP, CTP, GTP, 0.01  $\mu$ M of UTP, 0.5  $\mu$ l of 3000 Ci mmol<sup>-1</sup> [ $\alpha$ -<sup>32</sup>P] UTP and 0.5 U  $\mu$ l<sup>-1</sup> of RNasin (Promega). Final quantities of RNA/DNA templates were 100–150 ng. Reactions were initiated by adding 50–100 ng of SEC-purified MBP-RDR3 protein (or affinity-purified MBP-RDR3 for Fig. 8b–d, to be described later) or immunoprecipitated GFP-RDR3 protein and incubated at 25°C for 150 min. The reaction mixture was extracted with phenol:chloroform:isoamyl alcohol (25:24:1) and RNAs/DNAs were precipitated by ethanol precipitation. RNAs/DNAs were loaded on a denaturing urea-PAGE gel and visualised by phosphor imaging. As shown in Fig. 8(b–d) (described later), reaction products were directly loaded onto a denaturing urea-PAGE gel and visualised by phosphor imaging.



## Nuclease treatment

For RNase A treatment, purified reaction products (reconstituted in water) were treated with 0.5  $\mu\text{l}$  of 10 mg  $\text{ml}^{-1}$  RNase A (Thermo Fischer Scientific, Waltham, MA, USA) at 37°C for 25 min. For RNase I (Thermo Fischer Scientific) and RNase H (NEB) treatments, nuclease reactions were performed in RNase I buffer (50 mM Tris-HCl, pH 7.6, 15 mM  $\text{MgCl}_2$  and 600 mM NaCl) or 1 $\times$  RNase H buffer (75 mM KCl, 50 mM Tris-HCl, 3 mM  $\text{MgCl}_2$ , and 10 mM DTT), respectively. Treatment was initiated by adding 0.2  $\mu\text{l}$  of 10 U  $\mu\text{l}^{-1}$  RNase I or 5 U of RNase H followed by incubation at 37°C for 15 min (for RNase I) and 25 min (for RNase H).

## Results

### OsRDR3 and OsRDR4 belong to the $\gamma$ -clade of RDRs with an atypical catalytic motif

To establish a relationship between different clades of plant RDRs, we constructed a phylogenetic tree using RDR sequences derived from three different plant species. We found that RDR3, 4 and 5 (all  $\gamma$ -clade RDRs) formed a separate branch compared with RDR1, 2 and 6, all members of the  $\alpha$ -clade of RDRs (Fig. 1a).  $\gamma$ -Clade RDRs were also distinct between monocots and dicots. We aligned amino acid sequences of RDRs and found that there was a leucine to phenylalanine (L $\rightarrow$ F) substitution in the conserved catalytic domain of  $\gamma$ -clade RDRs such as in RDR3, 4 and 5, when compared with  $\alpha$ -clade members that had L in this position (Fig. 1b). Except for OsRDR1 and OsRDR3, all other RDRs were >1000 amino acids in length (Fig. 1c). Careful analysis of protein sequences suggested that  $\gamma$ -clade RDRs are more similar to each other when compared with their  $\alpha$ -clade counterparts that varied at the amino acid sequence level (Fig. 1d). This suggested a possible functional redundancy in functions among  $\gamma$ -clade RDRs. Both OsRDR3 and OsRDR4 are located on chromosome 1 in close proximity, suggesting a possible gene duplication event resulting in the formation of these members (Fig. 1e,g) (Kawahara *et al.*, 2013; Sakai *et al.*, 2013). Highest expression of OsRDR3 was observed in vegetative leaf and root tissues, while OsRDR4 expression was high in leaf and panicle tissues (Fig. 1f,h; Methods S1). This difference in expression indicated a possible neofunctionalisation. The expression profile of  $\gamma$ -clade RDRs in *indica* subspecies members is different from those in *japonica* rice, suggesting their potential to mediate different roles in these subspecies (Fig. S1). By contrast with  $\gamma$ -clade RDRs in rice, Arabidopsis  $\alpha$ -clade RDRs such as AtRDR1 were expressed at higher levels in older leaves and inflorescence apex, while AtRDR2 and AtRDR6 were consistently expressed at high levels in all tissues (Willmann *et al.*, 2011). Similarly, expression of  $\gamma$ -clade RDRs in rice is also ubiquitous, with a slightly higher expression seen in inflorescence tissues (Kapoor *et al.*, 2008), leaves and root tissues.

### Mis-expression of $\gamma$ -clade RDRs in transgenic rice altered growth and development

To find out the functional significance of  $\gamma$ -clade RDRs in *planta*, we generated OE and KD lines on the PB-1 background;

PB-1 is an elite *indica* rice line. For generation of OE lines of OsRDR3, we expressed the coding sequences under the maize ubiquitin promoter for constitutive high expression (Fig. 2a). The OsRDR3 OE plants had robust regeneration in selection media with robust callus formation (Fig. S2a,b), showing faster growth, increase in height and increased number of tillers, when compared with the controls (Figs 2a–c, S3e). We verified genome integration of RDR3 by junction fragment Southern analysis (Fig. S3a,b; Methods S2), and OE of the transgene was also verified by semiquantitative RT-PCR (Fig. S3c,d; Method S3). Interestingly, a transgenic line (#9) that had high expression of antibiotic resistance marker gene had OsRDR3 silenced, which was likely to be due to homology-dependent RNA silencing (Fig. S3c,d). This plant had poor growth and did not progress to the adult phase (Figs 2a, S3e). To observe the effect of downregulation of OsRDR3, we also generated KD lines of OsRDR3 using an amiR strategy as discussed in the Materials and Methods section (Schwab *et al.*, 2006; Warthmann *et al.*, 2008). These amiRs were incapable of targeting other closely related RDRs as they targeted unique motifs. The silencing of the *OsRDR3* gene was confirmed by RT-PCR in amiR-expressing silenced lines (Figs 2d, S3f). Similar to the line #9 described in Fig. 2(a) where OsRDR3 was silent, OsRDR3 amiR lines produced fewer leaves, the plant height and tiller numbers were drastically decreased and they did not progress beyond the vegetative phase (Figs 2d–f, S2c). Conversely, robust growth was also observed when OsRDR3 was heterologously expressed under the CaMV 35S promoter in tobacco (Fig. S4a–c). Taken together these results indicated that RDR3 overexpression increased plant growth while silencing of RDR3 was detrimental to plant growth.

Furthermore, to determine the significance of other  $\gamma$ -clade RDRs in rice, we also generated both overexpression and knock-down lines of another closely related protein of RDR3, OsRDR4 (Figs S5a–d, S6a–c; Methods S1, S4). Overexpression of OsRDR4 did not result in as vigorous a growth phenotype as that of OsRDR3 (Figs 3a–c, S5e,f), with these plants producing slightly higher numbers of seeds per panicle when compared with controls. However, this increase in yield was not statistically significant unlike the enhanced yield that was observed when OsRDR3 was overexpressed. Similarly, OsRDR4 KD lines were stunted, their heading dates were delayed, panicle length and the number of filled grain were drastically reduced (Fig. 3d–j). Together, these results indicated that OsRDR3 and OsRDR4 play an important role in rice growth and development to such an extent that mis-expression of these  $\gamma$ -clade members resulted in either enhanced growth or drastically poor growth. These phenotypes in silenced lines also indicated the likely absence of functional redundancy among  $\gamma$ -clade members in spite of having high sequence similarity. By contrast, such drastically altered phenotypes were not observed in Arabidopsis lines mis-expressing  $\alpha$ -clade RDRs, while silencing the RDR2 homologue in maize produced strong growth phenotypes (Jia *et al.*, 2009). Absence of strong phenotype in  $\alpha$ -clade RDR-silenced lines in Arabidopsis is striking especially as these genes control phenotypes ranging from vegetative phase change, lateral root production, cell identity, anthocyanin production and determination of leaf abaxial and adaxial polarity (Peragine *et al.*, 2004;

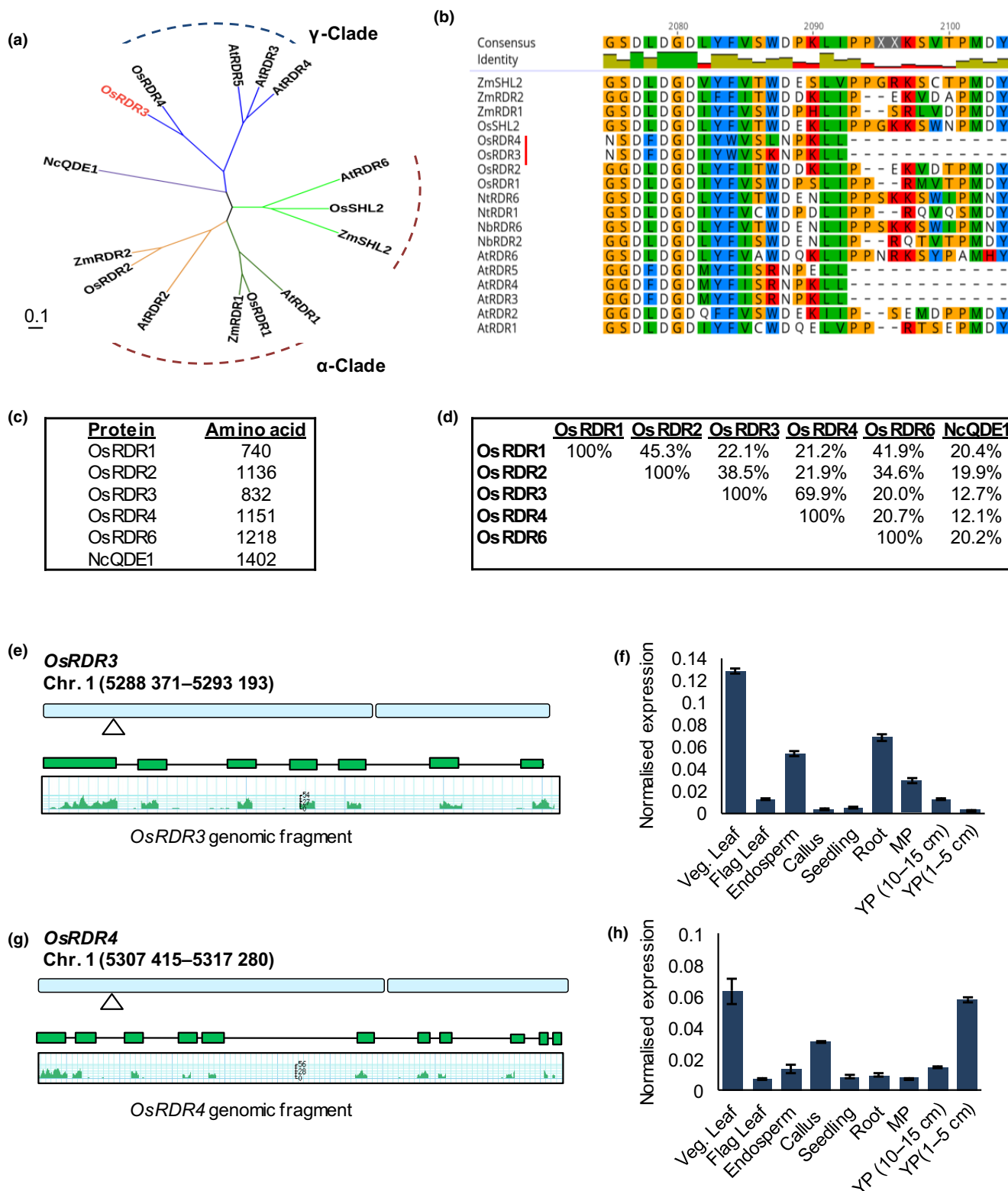


**Fig. 1** Sequence and expression analysis of rice RNA-dependent RNA polymerases (RDRs). (a) Phylogenetic analysis of selected  $\alpha$ -clade and  $\gamma$ -clade RDRs. (b) Amino acid sequence alignment of catalytic domain of  $\alpha$ - and  $\gamma$ -clade RDRs.  $\gamma$ -clade RDRs have a different catalytic motif compared with  $\alpha$ -clade RDRs. (c) Summary of protein sequence length of different rice RDRs. (d) Protein sequence similarity between different rice and *Neurospora* RDRs. Values are calculated in percentages. (e) Chromosomal location, exon positions and expression of OsRDR3. Green box represents the exons and solid black line represents the introns. Arrowhead indicates the gene location in the chromosome. The G-Browser picture was downloaded from RAP-DB. (f) Expression analysis of OsRDR3 across tissues of *Oryza sativa indica* by RT-qPCR. YP, young panicle; MP, mature panicle. OsACTIN1 was used as an internal control. The error bars indicate SE. (g) Chromosomal location, exon positions and expression of OsRDR4. The G-Browser picture was downloaded from RAP-DB. (h) Expression analysis of OsRDR4 across tissues of *O. sativa indica* by RT-qPCR. The error bars indicate SE.

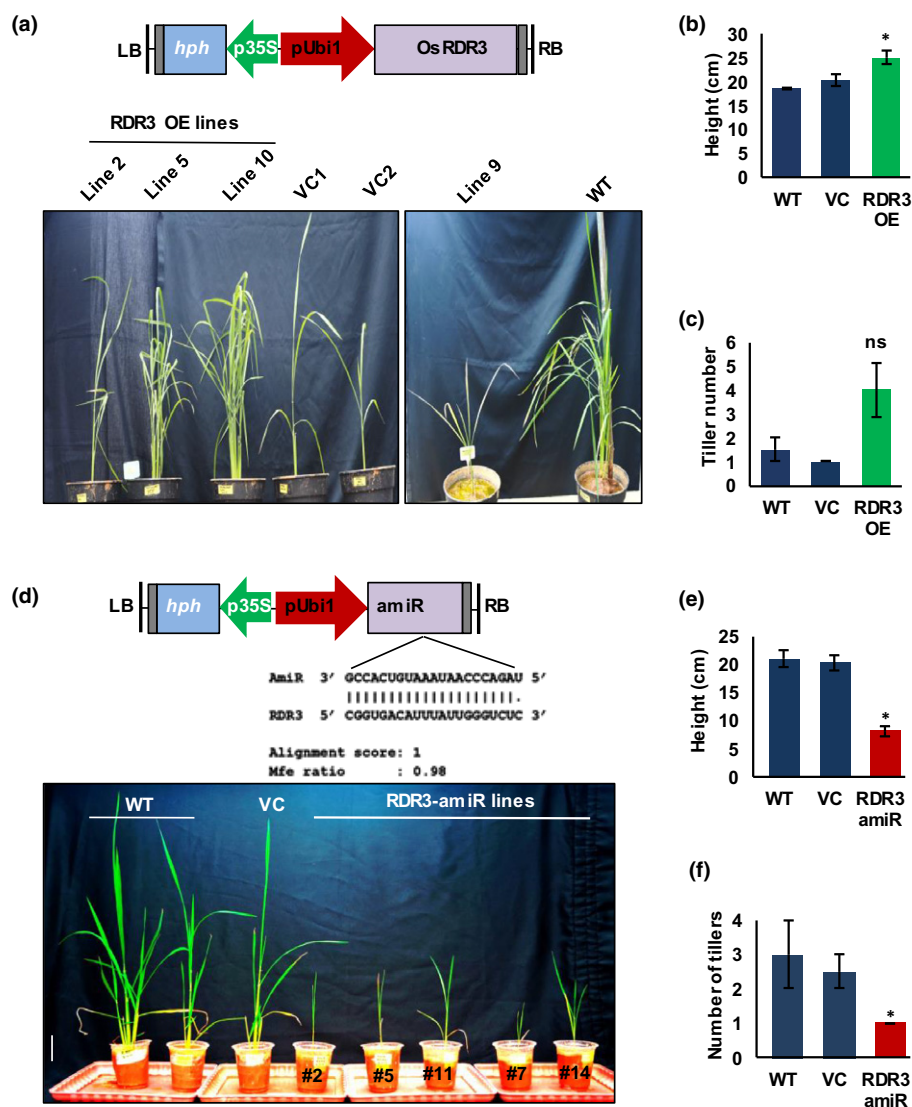


**Fig. 2** Phenotypic analysis of *OsRDR3* mis-expressing transgenic plants. (a) Phenotype of 70-d-old *RDR3* OE (lines #2, #5, #10) and homology-dependent KD (line #9) transgenic plants. (b, c) Measurements of height and tiller numbers in *RDR3* OE plants, respectively (\*,  $P < 0.05$ , one-tailed Student's *t*-test,  $n = 3$ , ns, nonsignificant). The error bars indicate SE. (d) Phenotype of 21-d-old *RDR3* amiR transgenic plants. Bar: 5 cm. (e, f) Height and tiller numbers of *RDR3* amiR plants, respectively (\*,  $P < 0.05$ , one-tailed Student's *t*-test,  $n = 4$ ). The error bars indicate SE. amiR, artificial miRNA; KD, knockdown; OE, overexpression; VC, vector-alone transformed control plant; WT, wild-type.

Chitwood *et al.*, 2009; Hsieh *et al.*, 2009; Schwab *et al.*, 2009; Marin *et al.*, 2010; Olmedo-Monfil *et al.*, 2010). Taken together, these observations reinforced the idea that plants with complex genomes and evolutionary histories have evolved diverse silencing pathways when compared with plants with smaller genomes. Functional diversity between recently duplicated, additional copies of silencing-associated genes have been characterised in monocot model plants (Nishimura *et al.*, 2002; Nagasaki *et al.*, 2007; Vaucheret, 2008; Wu *et al.*, 2009; Das *et al.*, 2020; Pachamuthu *et al.*, 2021).

*OsRDR3* alters the expression of various endogenous loci including those coding for proteins and noncoding sRNAs

As *OsRDR3* has a more drastic effect on rice growth and development when compared with *OsRDR4*, we further focused on

*OsRDR3* to decipher the role of  $\gamma$ -clade RDRs. As all RDRs are key components of RNA silencing, and as generation of dsRNA synthesised by RDRs is a key trigger for silencing, we explored if *OsRDR3* had specific targets for silencing in the rice genome. To identify targets of *OsRDR3*, we isolated sRNA and mRNA fractions from *RDR3* OE as well as the silenced line #9 and compared the RNA profiles with the controls. We obtained an average of 20 million (M) reads per sample in sRNA datasets and 20 M paired-end reads in RNA-seq datasets (Table S3). RNA-seq analysis identified differential expression of multiple genes in *RDR3* OE and KD lines when compared to WT plants (Fig. 4a, b; Datasets S1, S2). This analysis revealed that there were 917 and 1044 differentially expressed genes in *RDR3* OE and KD lines, respectively, indicating changes in gene expression when *OsRDR3* was mis-expressed (Fig. 4c). Gene ontology analysis identified enrichment of many important processes, such as

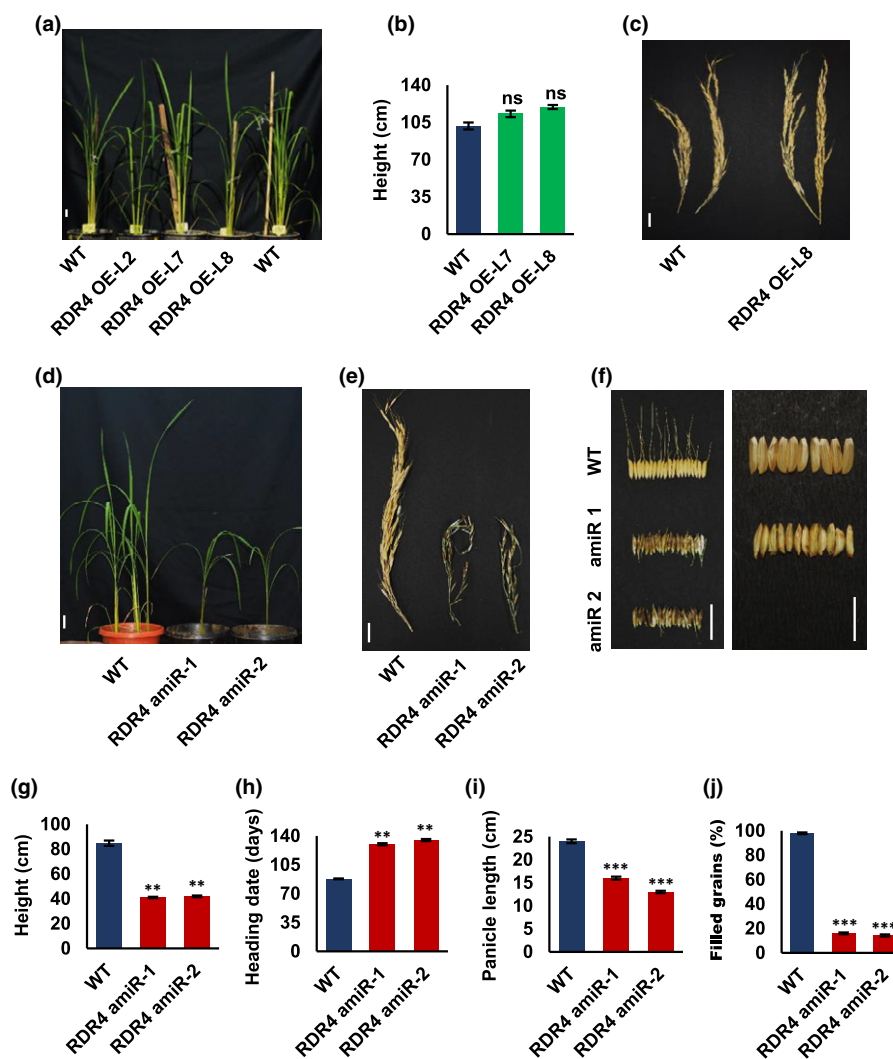


**Fig. 3** Phenotypic analysis of *OsRDR4* mis-expressing transgenic plants. (a) Phenotype of *OsRDR4* OE transgenic lines. Representative image of 8-wk-old wild-type (WT) and OE plants. Bar, 5 cm. (b) Plant height measurements of WT and *OsRDR4* OE lines. Error bars indicate SE. (c) Representative image of panicles of control and *OsRDR4* OE-Line 8. Bar, 2 cm. (d) Phenotype of *RDR4* amiR transgenic lines. Representative images of 7-wk-old WT and *T<sub>1</sub>* amiR plants. Bar, 5 cm. (e) Representative image of mature panicles of control and *RDR4* amiR lines. Bar, 2 cm. (f) Left: Representative image of seeds of control and *RDR4* amiR. Bar, 2 cm; Right: Representative image of de-husked seeds of control and *RDR4* amiR. Bar, 1 cm. (g–j) Measurements of plant height, heading date, panicle length and percentage of filled grains per panicle of control and *RDR4* amiR lines, respectively. Error bars indicate SE. Statistically significant differences between control and amiR lines were determined by Student's *t*-test (\*,  $P < 0.05$ ; \*\*,  $P < 0.01$ ; \*\*\*,  $P < 0.001$ ; ns, nonsignificant). amiR, artificial miRNA; OE, overexpression; WT, wild-type.

changes to cell wall synthesis genes, cell cycle-related genes, those responding to oxidative stress and many others that were differentially regulated in *RDR3* mis-expressed lines (Fig. 4d). These changes in gene expression were in agreement with the changes seen in host plants when other clades of RDRs were mis-expressed. In the *mop1* mutant of maize (*RDR2* homologue), transposons and protein-coding genes were mis-regulated. Surprisingly, RNA-directed DNA-methylation (RdDM) pathway players were also mis-regulated in *mop1* (Jia *et al.*, 2009). Localised alterations in DNA-methylation level and corresponding changes in expression of genes around such loci were reported in *osrdr1* (Wang *et al.*, 2014), whereas *AtRDR1* was not reported to be associated with RdDM. *AtRDR6* is involved in tasiRNA production and therefore indirectly regulated the expression of ARF genes. *AtRDR6* also indirectly regulated expression at

*RDR6*-dependent RdDM loci (Song *et al.*, 2012; Nuthikattu *et al.*, 2013). Although the extent of changes in transcriptome in *OsRDR3* mis-expressing lines is comparatively high, transcriptomic studies in mis-expressing lines of other members of RDRs in monocots is likely to assist in finding conserved targets of such RDRs and their functional significance. Together, these results pointed out that the role of *OsRDR3* is to regulate host gene expression, directly or indirectly, to an extent similar to RDR family members of the well studied  $\alpha$ -clade.

*OsRDR3* mis-expressed lines also showed altered populations of sRNAs. sRNA profiling and 5'-nt bias comparison identified higher abundance of 24-nt reads in *RDR3* OE plants (Fig. 5a). There was also an increased percentage of 21-nt reads with a bias for 5' U in OE lines when compared with KD lines (Fig. 5b). Differential expression analysis of miRNAs revealed that



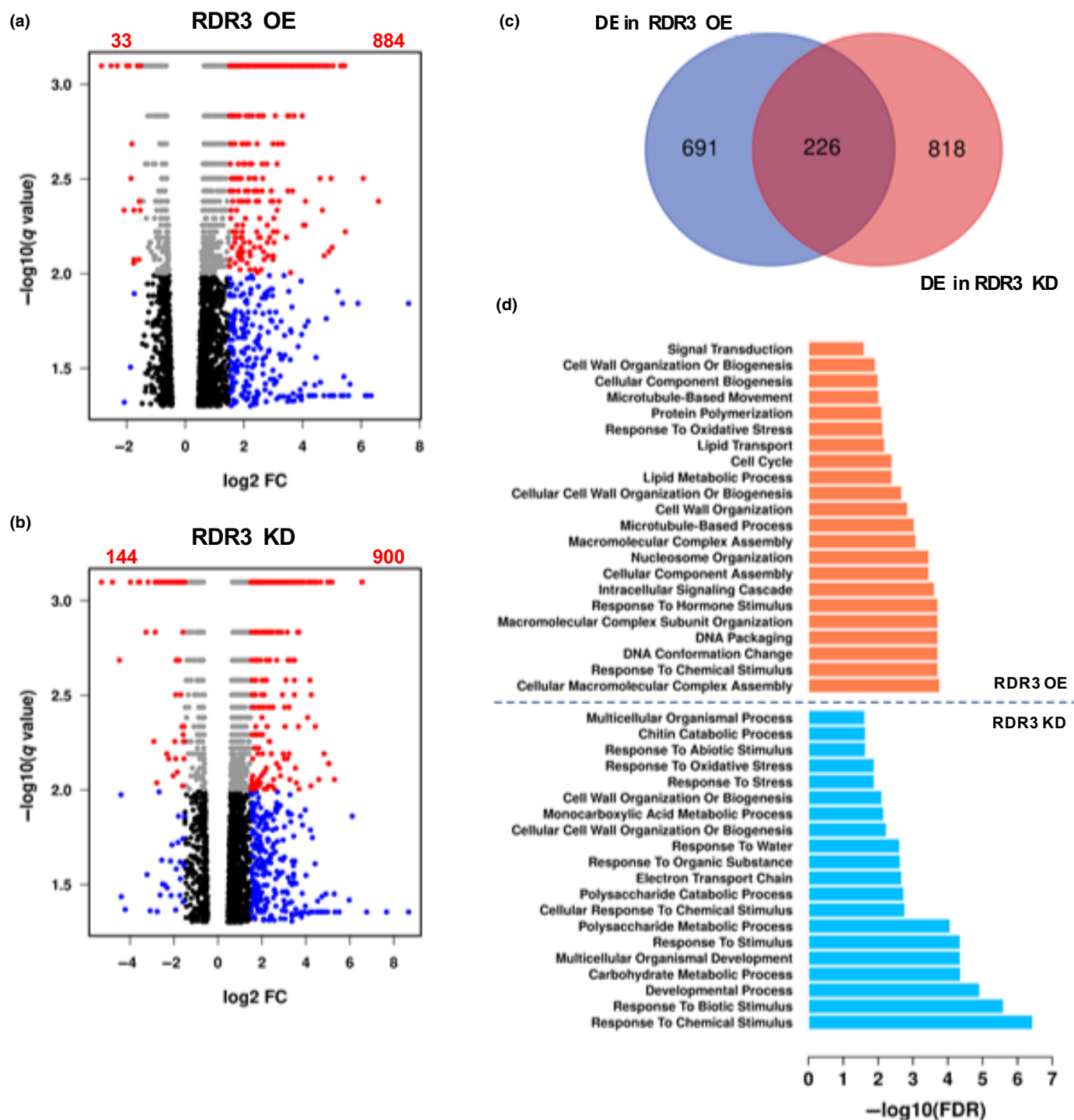


**Fig. 4** RNA-seq analysis of *OsRDR3* mis-expressing lines. (a, b) Volcano plots representing differentially expressed genes in RDR3OE (a) and RDR3KD (b), respectively. See the Materials and Methods section for details. (c) Venn diagram detailing number of differentially expressed genes overlapping between RDR3 OE and RDR3 KD lines. (d) GO enrichment of biological processes among the differentially expressed genes in RDR3 mis-expression lines. KD, knockdown; OE, overexpression.

expression of many miRNAs (e.g. miR166 and miR2118) were altered in RDR3 mis-expression lines (Fig. 5c). When we analysed the expression levels of corresponding targets of these miRNAs, obtained from degradome analysis, we observed an inverse correlation (Fig. 5d). miR1432, miR398 and miR408

that regulate yield-related or stress tolerated genes were upregulated in KD lines. These miRNAs when present at higher levels, reduced the yield and tolerance to stress among plants. miR1432 when overexpressed caused a reduction in acyl-CoA thioesterase (ACOT) levels thereby lowering the yield (Zhao *et al.*, 2019).



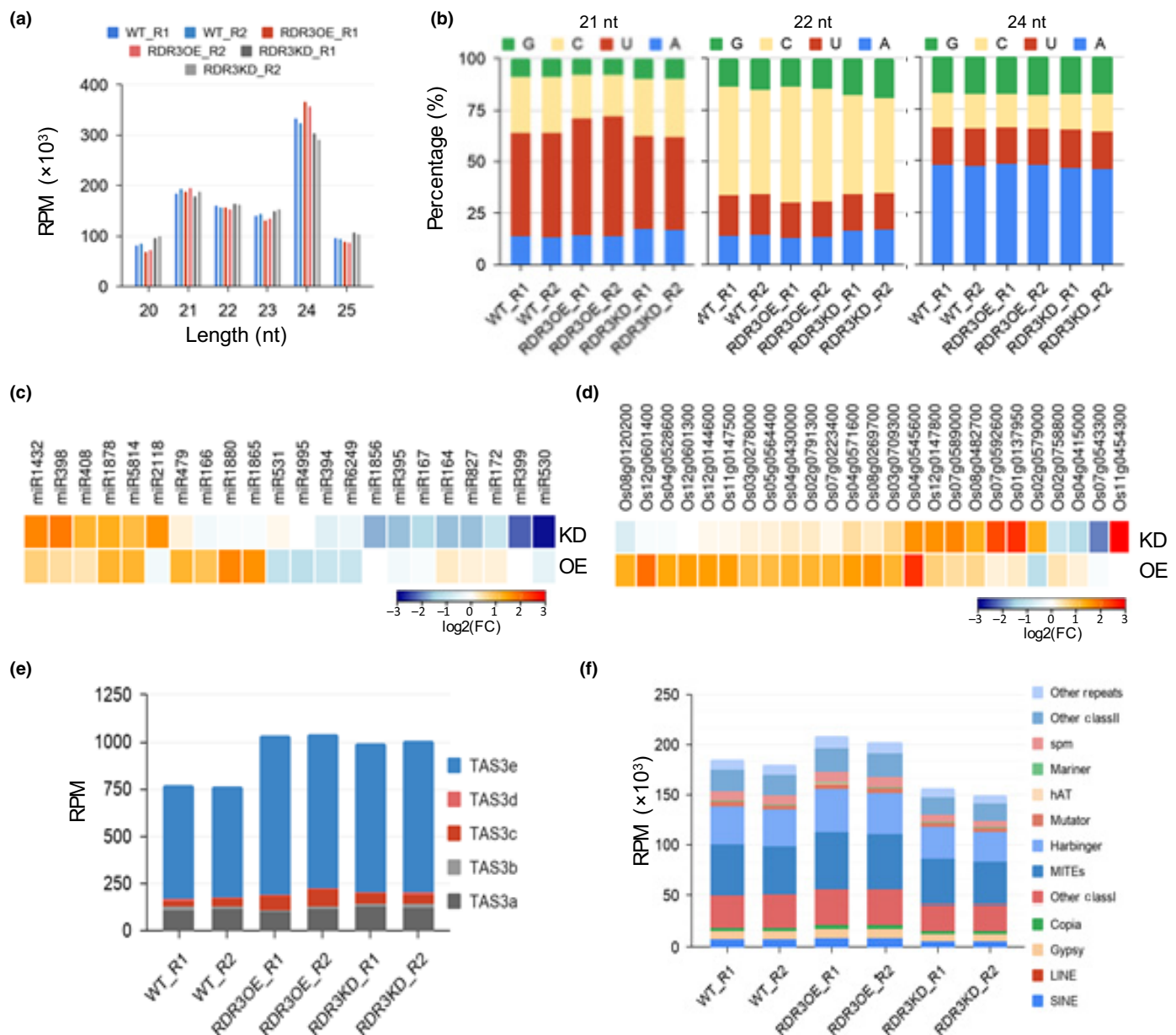


**Fig. 5** sRNA-seq analysis of *OsRDR3* OE and KD lines. (a) Size-class distribution of sRNAs in WT, RDR3 OE and RDR3 KD lines, represented as bar graphs. R1 and R2 are biological replicates. (b) 5'-nucleotide abundance profile of 21-nt, 22-nt and 24-nt sRNAs in three samples including replicates. (c) Heatmap of differentially expressing miRNAs in RDR3 OE and RDR3 KD, represented as log<sub>2</sub> (fold change) values. (d) Heatmap of differentially expressed miRNA targets in RDR3 OE and RDR3 KD represented as log<sub>2</sub> (fold change) derived from RNA-seq analysis. (e) Stacked-bar plot representing sRNA abundance in TAS3 loci in three samples. (f) Stacked-bar plot representing percentage abundance of sRNAs (20–25 nt) in genomic repeat loci. KD, knockdown; OE, overexpression; WT, wild-type.

miR398 and miR408 that target CSD1/2 and UCL8 respectively, are normally downregulated in stress so that their targets are upregulated to confer stress tolerance (Sunkar *et al.*, 2006; Lu *et al.*, 2011; T. Zhang *et al.*, 2017). Also, among the upregulated miRNAs in KD lines was miR2118, which regulates reproductive development in rice (Komiya *et al.*, 2014; Das *et al.*, 2020). Among the miRNAs downregulated in RDR3 KD lines was miR167 that targets OsARF12, OsARF17 and OsARF25. These genes control tiller angle (Li *et al.*, 2020). Similarly, miR164 that targets OsCUC1, which is required for boundary establishment

and maintenance during differentiation (Wang *et al.*, 2021), miR172 that targets INB and OsIDS1, two members of the AP2 family that control floral organ identity and development (Lee & An, 2012), miR399 that targets LTN1, takes part in regulating phosphate starvation response in rice (Hu & Chu, 2011), miR530 whose target is PL3, which encodes a PLUS3 domain-containing protein (Sun *et al.*, 2020) were downregulated in KD lines. Among the miRNAs that were upregulated only in RDR3 OE was miR166 that targets HD-ZIPIII TFs, regulators of growth, vascular development, and establishment of leaf polarity

(Mallory *et al.*, 2004; Kim *et al.*, 2005; Williams *et al.*, 2005; J.-P. Zhang *et al.*, 2017). It is tempting to speculate that the mis-expression of these miRNAs might have contributed to the poor development of OsRDR3 and OsRDR4 KD lines. To find out if RDR3 played a role in tasiRNA biogenesis similar to AtRDR6, we compared abundance of well conserved TAS3-derived siRNAs (Fig. 5e), as well as 21-nt and 24-nt siRNAs from PHAS loci across samples (Fei *et al.*, 2016; Tables S4, S5), and observed that OsRDR3 also influenced their accumulation. To identify if functions of OsRDR3 overlapped with RDR2, we compared sRNA abundance in repeat and transposon loci that are usually under the influence of RDR2 or its homologues and observed that RDR3 OE plants accumulated increased amounts of these siRNAs, whereas KD lines had reduced accumulation (Fig. 5f). Together, these results indicated that RDR3 is involved in the production of sRNAs in several genomic loci, probably by directly acting on specific loci or indirectly acting by competing with other clades of RDRs.

### OsRDR3 regulates the expression of repeat-rich regions in rice genome

To identify the loci responsible for altered abundance of sRNAs in RDR3 OE/KD lines, we compared the expression of sRNA loci between these datasets. Among the loci that had differential expression in RDR3 OE and KD lines, there was an enrichment of genic regions and miRNAs (Fig. 6a,b). Among the 24-nt class, repeats of class I (2.40% in RDR3 OE compared with 2.25% in RDR3 KD for 20–22-nt; and 14.95% in RDR3 OE compared with 10.84% in RDR3 KD for 23–24-nt) and class II (5.10% in RDR3 OE compared with 4.20% in RDR3 KD for 20–22-nt; and 35.15% for RDR OE compared with 26.83% for RDR3 KD for 23–24-nt) showed major changes in accumulation. In addition, there were changes in other repeats (0.40% in RDR3 OE compared with 0.32% in RDR3 KD for 20–22-nt; and 3.53% for RDR3 OE compared with 2.60% for RDR3 KD for 23–24-nt), transposons and rRNA repeats (47.29% in RDR3 OE compared with 54.27% in RDR3 KD for 20–22-nt and 26.74% in RDR3 OE compared with 37.01% in RDR3 KD for 23–24-nt) (Figs 6a,b, S7a). Together, among the loci that had differential expression, loci derived from rRNA, rRNA repeats, class I and class II repeats were the major loci responsible for the differential expression of sRNAs (Figs 6c,d, S7b). In all such cases, expression of sRNA from the coding sequences were not altered (Fig. 6e) suggesting that OsRDR3 is specifically generating sRNAs from repeat-rich regions in rice genome. While there was no significant difference in the sRNA derived from rRNA repeats in RDR4 mis-expressing transgenic plants, similar to RDR3, repeats and transposons had altered accumulation (Fig. S8a,b), suggesting that RDR3 and RDR4 might have somewhat similar roles in genome regulation. Differential expression analysis of sRNA loci suggested that there were 1124 and 1007 differentially expressed sRNA loci in RDR3 OE and KD lines, respectively (Fig. 6f; Dataset S3). Three representative transposon loci with higher abundance of sRNAs in OE plants and lower in KD plants are shown in Fig. 6(g–i). Many genomic loci, where

OsRDR3 acted on the specific regions have been summarised in Figs S10–S13. These results suggested a likely involvement of OsRDR3 in a pathway partly catalysed by RDR2 in Arabidopsis and other model systems, where RDR2 plays a major role in converting PolIV-derived transcripts from repeats and transposon-rich regions to dsRNAs so that DCL3 generates a pool of 24-nt sRNAs. These signals are utilised to induce DNA-methylation and histone modifications in model plants such as Arabidopsis. To identify if other component of RNA silencing pathway, such as DCLs, RDRs of other clades and AGOs, have an effect or contribution to RDR3-dependent loci, we overlapped RDR3-dependent loci with publicly available datasets and found that components of the RdDM pathway influenced the sRNA abundance at these loci (Fig. S9a,b). Strikingly, there was biased accumulation of sRNAs in one strand as well as enhanced expression of the gene in OsRDR3 plants, such as in a long terminal repeat (LTR) element (Fig. S10c) and protein-coding genes (Figs S11b, S12d, S13). In most such cases, genomic regions had multiple repeats spanning the gene (Fig. S13). In a few cases, KD of OsRDR3 induced the expression of genomic loci to produce long RNAs as well as abundant 21-nt and 24-nt sRNAs (Fig. S12c). In the examples provided in Fig. S12, repeats in which OsRDR3 played a role in enhancing or reducing abundance of sRNAs also altered the expression of neighbouring genes as seen in RNA-seq. In most examples mentioned above, the changes were mostly in 24-nt sRNAs in OsRDR3 mis-expressing lines. In all such examples, lengths of differentially expressing sRNA loci were shorter, spanning 100–300-bp regions. Taken together, these examples indicated a profound implication of mis-expression of OsRDR3 in gene expression and the ability of OsRDR3 to alter the normal pool of sRNAs. In a small subset of regions where OsRDR3 appeared to act as a DdRp, it is possible that OsRDR3 itself is capable of generating dsRNAs or that these ssRNAs might be used as substrates by other members of RDRs.

To verify if OsRDR3 is capable of generating substrates from repeats and transposons in a heterologous system, we checked the expression of *Tto1* (an LTR retrotransposon, class I) in RDR3 OE transgenic *N. tabacum* plants. We found that the expression of *Tto1* was increased in RDR3 OE plants when compared with vector-alone transformed control plants (Fig. S4d). These results indicated that OsRDR3 has specific polymerase functions for efficient targeting of repeat-rich regions in the genome.

### RDR3 has polymerase activity on both RNA and DNA templates

We hypothesised that, similar to  $\alpha$ -clade member AtRDR6,  $\gamma$ -clade members of RDRs might have specific polymerase activities to mediate sRNA biogenesis from specific genomic loci. To study the biochemical properties of OsRDR3, we amplified a 2.5-kb full-length OsRDR3 coding for 832 amino acids and cloned it into a modified pMAL-p5E expression vector designed for a translational fusion of MBP at the N-terminal end (Fig. S14a). The MBP–RDR3 construct was then transformed into C41 *E. coli* expression cells and the protein was purified by affinity chromatography using dextran–sepharose beads at 4°C

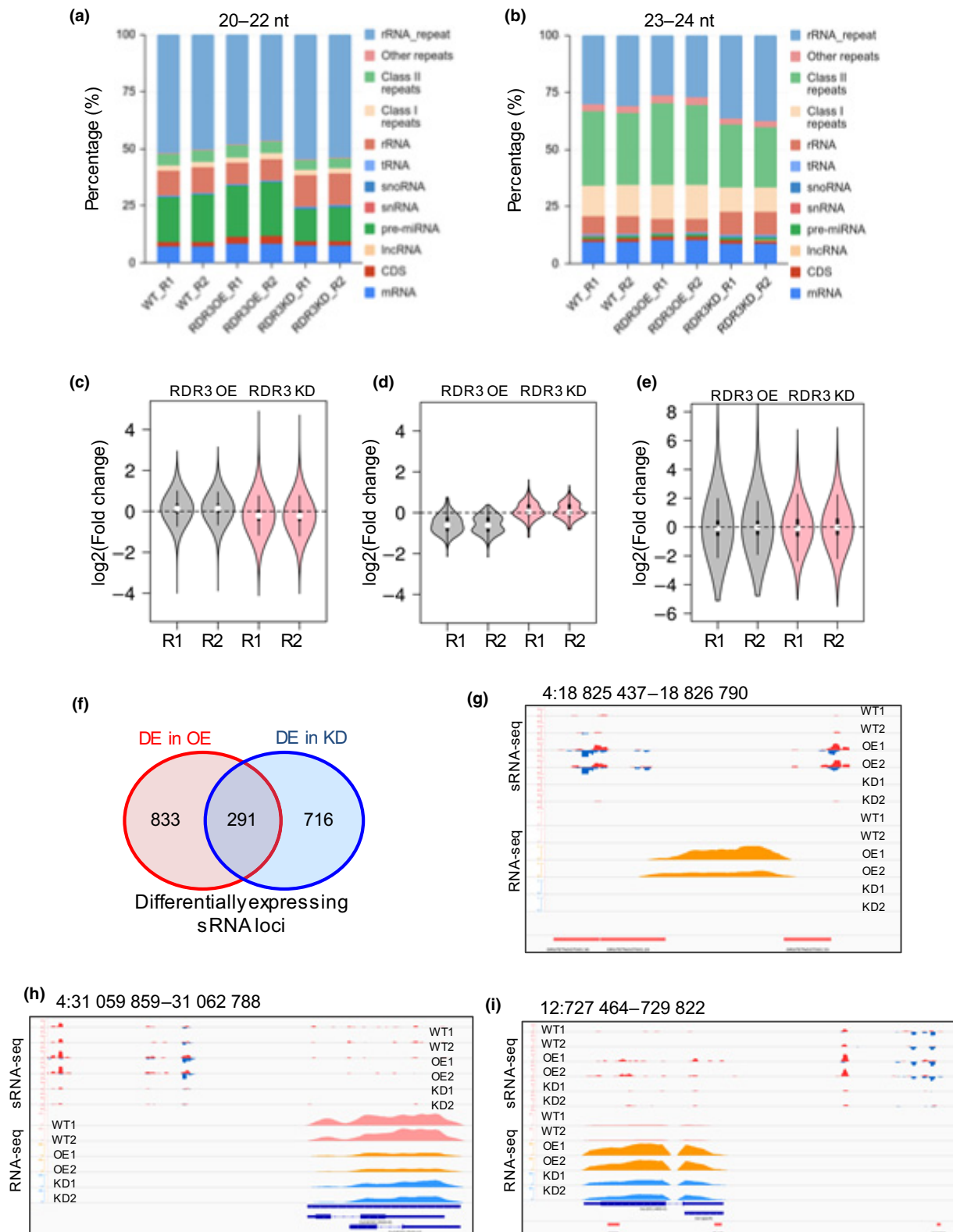


**Fig. 6** sRNA abundance among *OsRDR3* mis-expressing lines in various genomic features. (a) Stacked-bar plot representing percentage abundance of sRNAs (20–22 nt) in various genomic features. (b) Stacked-bar plot representing percentage abundance of sRNAs (23–24 nt) in various genomic features. (c) Violin plot representing log<sub>2</sub> (fold change) of sRNA abundance in RDR3 OE and RDR3 KD in repeat loci (23–24 nt). (d) Violin plot representing log<sub>2</sub> (fold change) of sRNA abundance in RDR3 OE and RDR3 KD in rRNA repeat loci (20–25 nt). (e) Violin plot representing log<sub>2</sub> (fold change) of sRNA abundance in RDR3 OE and RDR3 KD in coding sequence (CDS) loci (20–25 nt). (f) Venn diagram representing overlap of differentially expressed sRNA loci between two RDR3 mis-expressing lines. (g–i) Examples of differentially expressing loci. KD, knockdown; OE, overexpression; WT, wild-type.

(Fig. S14b–e). The protein was further purified by SEC using a HiLoad Superdex 200 pg preparative SEC column (GE Healthcare) (Fig. 7a). Expression of the MBP–RDR3 fusion protein was further confirmed by western blot analysis (Fig. 7a) and mass spectrometry analysis.

To explore the polymerase activities of OsRDR3 on ssRNA substrates, a 60-nt long ssRNA template corresponding to the 853–912-nt region of eGFP was used as a template in the presence of [ $\alpha$ - $^{32}$ P] UTP and all four cold rNTPs. We found that RDR3 was able to form RNAs of correct length from the ssRNA template (Fig. 7b). As expected, activity was not observed in the reaction using MBP as a vector control. To verify that newly formed products were genuine RNAs, we digested the reaction products with RNase A and degradation of this RNA confirmed the production of new RNAs (Fig. 7b). We further treated the reaction products with RNase I that had affinity for ssRNAs but not for dsRNAs, and observed the signal even after treatment with RNase I, suggesting that the newly formed product was the expected RNA:RNA hybrid (Fig. 7b). Substrate specificity of RNase A and RNase I is shown in Fig. 7(c). Together, these results suggested that OsRDR3 has robust primer-independent polymerase activity on ssRNA substrates. These biochemical properties of OsRDR3 were similar to previously reported activities for AtRDR6 and AtRDR2 (Curaba & Chen, 2008; Devert *et al.*, 2015).

It has been shown previously that  $\alpha$ -clade RDRs have nucleotidyl transferase activity on ssRNA substrates (Curaba & Chen, 2008). Viral RdRps are also known to possess this activity, although its significance is unknown (Ranjith-Kumar *et al.*, 2001; Kim *et al.*, 2007). We explored if OsRDR3 also had nucleotidyl transferase activity on ssRNA substrates. We incubated OsRDR3 with ssRNA in the presence of only [ $\alpha$ - $^{32}$ P] UTP or CTP. We detected a band of the correct size in reactions with only [ $\alpha$ - $^{32}$ P] UTP or CTP, suggesting that RDR3 has nucleotidyl transferase

activity on ssRNA (Fig. 7d). In these activities, OsRDR3 behaved very similarly to AtRDR6.

During the protein sequence alignment of  $\gamma$ -clade RDRs with other DNA-dependent RNA polymerases we observed that the DFDGD motif was conserved throughout the DNA-dependent RNA polymerase family. As OsRDR3 has such a motif, we explored if OsRDR3 was capable of using DNA as a template for RNA synthesis. To test this, we incubated OsRDR3 with a 74-nt long ssDNA with [ $\alpha$ - $^{32}$ P] UTP and all four cold rNTPs. We found that OsRDR3 was able to synthesise RNAs of correct size from ssDNA (Fig. 8a). To understand the nature of this newly synthesised RNA, we digested the reaction products with RNase H that degrades RNA from the DNA:RNA hybrid, and observed that the RNA product was sensitive to RNase H. This suggests that newly formed RNA was a hybrid of DNA:RNA (Fig. 8a). As expected, we did not observe any signal in a reaction with MBP used as a control. We observed that RDR3 required  $Mg^{2+}$  ions for its polymerase activity, similar to other polymerases (Fig. 8b). Among the ranges of temperatures tested, it worked best at a slightly higher temperature range 20–40°C (Fig. 8c). Its requirement of a slightly basic pH for its optimum activity is in a similar range as observed with other RDRs (Fig. 8d).

#### Mutation in conserved catalytic domain partially reduces the polymerase activity of OsRDR3 *in vitro*

It has been shown previously that mutations in the conserved catalytic domains of  $\alpha$ -clade RDRs and viral RdRps (DXDXD-eukaryotic; DX<sub>4-5</sub>D or DXD-viral) abolished their polymerase activities (Jablonski & Morrow, 1995; Curaba & Chen, 2008; Ogden *et al.*, 2012; Devert *et al.*, 2015). To check whether this motif was also essential for the polymerase activity of  $\gamma$ -clade RDRs, we generated a mutant in the conserved DFDGD

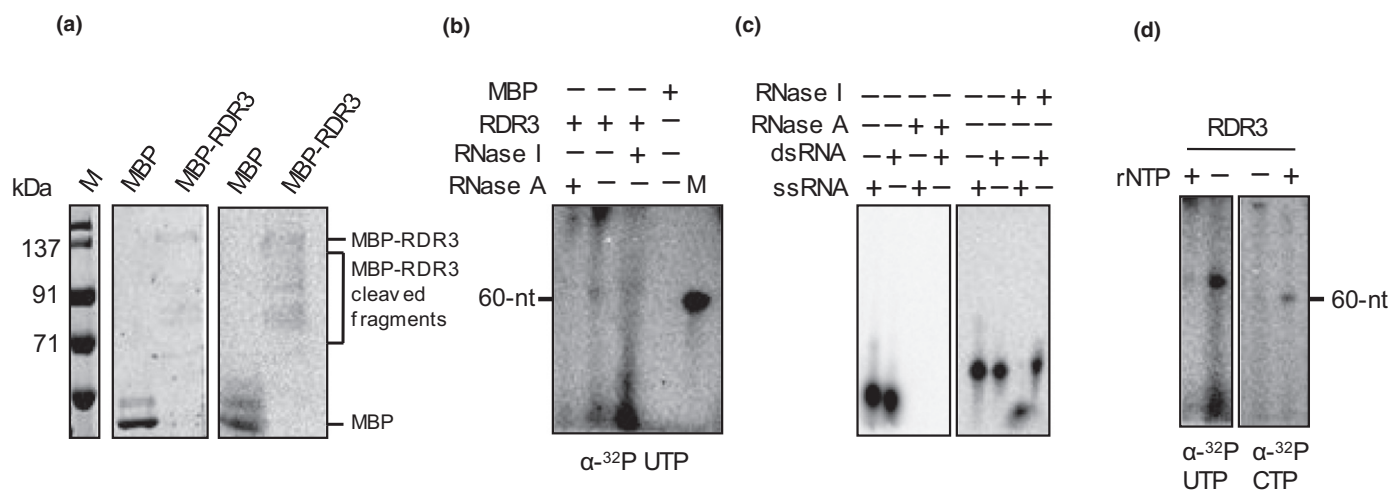


**Fig. 7** Polymerase activity of OsRDR3 on ssRNA substrates. (a) Coomassie Brilliant Blue staining (left) and western blotting (right) of purified MBP-RDR3 protein after size exclusion chromatography. (b) *In vitro* RNA-dependent RNA polymerase (RDR) assay for RDR3 on a 60-nt long ssRNA template in the presence of cold rNTPs and radiolabelled UTP. Reaction products were separated on a 12% urea-PAGE gel and visualised by phosphor imaging. 5-end labelled 60-nt RNA was used as a size marker. (c) Nuclease activity of RNase A and RNase I on a 21-nt long ssRNA and dsRNA substrates. (d) RDR activity of RDR3 on a 60-nt ssRNA template in the presence or absence of cold rNTPs with radiolabelled UTP or CTP. Reaction products were separated on a 12% urea-PAGE gel and visualised by phosphor imaging. CTP, cytidine triphosphate; ds, double stranded; rNTP, ribonucleoside triphosphates; ss, single stranded; UTP, uridine triphosphate.



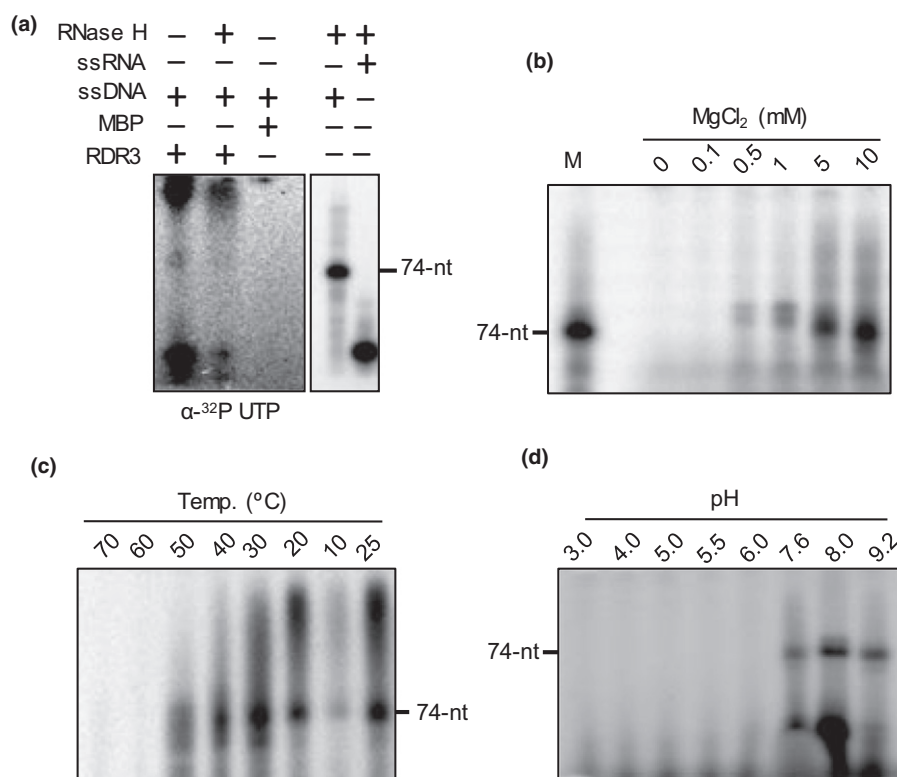


**Fig. 8** Polymerase activity of OsRDR3 on ssDNA substrates. (a) RDR3 polymerase assay with a 74-nt ssDNA template. Reaction products were either treated or not with RNase H. 5'-end labelled template DNA was used as a marker. Reaction products were resolved on a 12% urea-PAGE gel. Right panel shows the specificity of RNase H towards DNA:RNA hybrid. ss, single stranded; ds, double stranded. (b) Cation requirement for RDR3 polymerase activity. Polymerase assay was performed with varying concentrations of MgCl<sub>2</sub> on a ssDNA template with an affinity-purified protein. Reaction products were resolved on a 15% urea-PAGE gel. (c) Optimum temperature required for RDR3 activity. Polymerase assay was performed at different temperatures in the presence of radiolabelled UTP and cold rNTPs with affinity-purified protein. (d) Optimum pH requirement for RDR3 polymerase activity. Polymerase reactions were performed in buffers at different pH in the presence of radiolabelled UTP and cold rNTPs with affinity-purified protein.

domain. The mutant had a substitution at the 693<sup>rd</sup> residue from aspartic acid (D) to alanine (A) (Fig. S14f,g). We purified the protein using affinity chromatography coupled with SEC and verified by western blotting with anti-MBP antibody (Fig. S14h, i). We found that mutating D→A partially abolished the OsRDR3 activity on ssDNA and ssRNA templates (Fig. S14j). To verify the activity of the RDR3 D693A mutant, we further immunoprecipitated WT and D693A mutant RDR3 from GFP-RDR3 and GFP-RDR3 D693A-overexpressing *N. tabacum* plants using either GFP-trap or GFP-nanobody (Fig. S15a–d; Methods S5–S7). In both the cases, we found that the RDR3 mutant was active at reduced levels (Fig. S15e,f). These results suggested that either there were other residues responsible for its activity or that its activity depended on multiple domains, similar to the observations in *Thermus aquaticus* and adenovirus DNA polymerase (Patel & Loeb, 2000). Together, our results indicated atypical activities of γ-clade members of RDRs in controlling gene expression through sRNAs.

## Discussion

sRNAs are master regulators of gene expression, involved in a multitude of functions in development, resistance and genome integrity across eukaryotes (Baulcombe, 2004; Voinnet, 2008).

The majority of the sRNAs arise from dsRNA intermediates that act as triggers to generate sRNAs from both endogenous and exogenous sources (Voinnet, 2008). RDRs generate dsRNAs from diverse substrates and it is of great significance to understand the functions of these enzymes. Previous sequence analysis of RDRs has indicated that γ-clade RDRs that are restricted to plants and fungi have unique motifs (Wassenegger & Krczal, 2006; Willmann *et al.*, 2011). Our analysis of RDRs from plants also reinforced the idea that γ-clade members are essential for the growth and development of plants.

Sequences of RDRs within a clade are highly variable; significance of which is unknown. For example, there is only a 39.1% amino acid sequence similarity between AtRDR3 and OsRDR3. There is only 36.5% similarity between AtRDR4 and OsRDR4 at the amino acid level. However, among the γ-clade members of one species, there is a high degree of similarity, for example, OsRDR3 and OsRDR4 share 70.7% similarity between them. It is likely that OsRDR3 and OsRDR4 are the result of a recent duplication event. Differential expression of OsRDR3 and OsRDR4 across different tissues highlighted a specific spatio-temporal regulation and their requirements in different tissues. We have also found different splice variants of OsRDR3, indicating further layers of regulation that might be important for rice development.

The vigorous growth of OsRDR3 OE transgenic rice and tobacco and stunted growth of OsRDR3 and OsRDR4 KD lines suggests an important role of these genes in the growth and development of plants. OE of AtRDR2, AtRDR6 or AtRDR1 did not lead to drastic changes in plant development (Curaba & Chen, 2008), indicating that a different regulatory aspect is associated with  $\gamma$ -clade RDRs. sRNA sequencing further revealed that there was an increase in the production of sRNAs from transposons and repeat-rich loci in OE lines and the reduction of these species in KD lines. This suggests efficient silencing of the transposons and repeats in OsRDR3, and to some extent OsRDR4, OE plants. This might allow expression and accumulation of RNAs that code for specific regulators of plant growth and development. Considering the robust DdRp activity of OsRDR3, it is possible that it might function together with PolIV or PolV. It has been reported previously that there are several classes of sRNAs that are independent of RDR1, 2 and 6 (Polydore & Axtell, 2018). We hypothesised that the  $\gamma$ -clade RDRs might also be regulating the production of such sRNAs however, as these loci have not been mapped in rice, we were unable to explore this possibility. Considering a previous report on the DFDGD class of RDRs in tomato (Verlaan *et al.*, 2013; Butterbach *et al.*, 2014), it might be possible that RDR3 is also involved in silencing of DNA viruses. OsRDR3 might help in making sRNAs from invading DNA viruses thereby contributing to their silencing and host defence.

Like AtRDR6, OsRDR3 also can use ssDNA as a template for RNA synthesis. Also on ssDNA templates it forms RNA of the correct size (Curaba & Chen, 2008). Considering that DFDGD motifs are also conserved throughout the DdRp family, it is possible that RDR3 might have evolved specifically as a DdRp rather than an RdRp. Aspartic acid in the conserved catalytic motif of plant RDRs is essential for their catalytic activity (Curaba & Chen, 2008; Devert *et al.*, 2015), however we were not able to identify a single motif/residue that is completely responsible for the catalytic activity of RDR. As it is a large protein there might be a possibility of having another catalytic motif responsible for polymerase activity or RDR3 might be interacting with subunits of other polymerases. As other studied RDRs also show primer-independent and sequence-independent activities, it is not surprising that OsRDR3 also performs similarly. For  $\alpha$ -clade RDRs such as AtRDR6, it has been shown that specificity for substrates of tasiRNA biogenesis is due to the specificity of the RDR partner protein SGS3 (Peragine *et al.*, 2004; Fukunaga & Doudna, 2009; Kumakura *et al.*, 2009). It is likely that partners of OsRDR3 mediate the recognition and polymerisation of substrates to initiate silencing of specific genomic regions. Our analysis also indicated a likely DdRp activity of OsRDR3 on specific repeat-rich substrates and this might also require a partner protein to help with recognition of such targets.

The results discussed above are interesting for several reasons. Growth and development-associated phenotypes of OE and KD of these RDRs confirmed the importance of  $\gamma$ -clade RDRs. This clade of RDRs appeared to be fully functional unlike in Arabidopsis, and they play a key role in genome regulation possibly through silencing of specific repeat-rich regions. These results

also showed that  $\gamma$ -clade RDRs possess atypical biochemical activities.







## Acknowledgements

The authors acknowledge access to sequencing, the mass spectrometry facility, glasshouse and radioactivity facility at NCBS. Thanks to Professor K. Veluthambi for *Agrobacterium* strain LBA4404 (pSB1), vectors and PB1 seeds. This work was supported by NCBS-TIFR core funding through the Department of Atomic Energy, Government of India, under Project Identification No. RTI 4006 (1303/3/2019/R&D-II/DAE/4749 dated 16 July 2020), and grants (BT/PR12394/AGIII/103/891/2014; BT/IN/Swiss/47/JGK/2018-19; BT/PR25767/GET/119/151/2017) from the Department of Biotechnology, Government of India. STN, SC, AN and KP acknowledge a fellowship from DBT, India. These funding agencies did not participate in the designing of experiments, analysis or interpretation of data, neither in the writing of the manuscript. Authors declare that they have no conflict of interest. Authors wish to dedicate this work to Prof. M. Udayakumar.

## Author contributions

PVS designed the study. VJ made recombinant constructs, produced the phylogenetic tree, carried out sequence alignment and performed all the biochemical assays. DB and STN generated and analysed transgenic rice plants. A. Narjala and SC performed bioinformatic analysis. KP generated GFP-RDR3 *N. tabacum* transgenic plants and performed RT-qPCR. A. Nair helped with assays. VJ and PVS analysed the data and wrote the manuscript.

## ORCID

Swetha Chenna  <https://orcid.org/0000-0002-9336-0798>  
Vikram Jha  <https://orcid.org/0000-0003-0731-3133>  
Ashwin Nair  <https://orcid.org/0000-0003-1338-5344>  
Anushree Narjala  <https://orcid.org/0000-0003-1772-4876>  
Padubidri V. Shivaprasad  <https://orcid.org/0000-0002-9296-4848>  
Sujith T. N.  <https://orcid.org/0000-0003-2715-6454>

## Data availability

RNA-seq and sRNA datasets related to this project have been deposited in the Gene Expression Omnibus. They can be accessed through GSE115053 (OsRDR3 RNA-seq), GSE115056 (OsRDR3 sRNA-seq) and GSE181778 (OsRDR4 sRNA-seq). Uncropped images of the gels are provided in Figs S16 and S17.

## References

- Adenot X, Elmayan T, Lauressergues D, Boutet S, Bouché N, Gascioli V, Vaucheret H. 2006. DRB4-dependent TAS3 trans-acting siRNAs control leaf morphology through AGO7. *Current Biology* 16: 927–932.
- Allen E, Xie Z, Gustafson AM, Carrington JC. 2005. microRNA-directed phasing during trans-acting siRNA biogenesis in plants. *Cell* 121: 207–221.

- Astier-Manificat S, Cornuet P. 1971. RNA-dependent RNA polymerase in Chinese cabbage. *Biochimica et Biophysica Acta (BBA) – Nucleic Acids and Protein Synthesis* 232: 484–493.
- Astier-Manificat S, Cornuet P. 1978. Purification and molecular weight of an RNA-dependant RNA polymerase from *Brassica oleracea* var. *botrytis*. *Comptes Rendus Hebdomadaires des Seances. Serie D. Sciences Naturelles* 287: 1043–1046.
- Baulcombe D. 2004. RNA silencing in plants. *Nature* 431: 356–363.
- Blevins T, Podicheti R, Mishra V, Marasco M, Wang J, Rusch D, Tang H, Pikaard CS. 2015. Identification of Pol IV and RDR2-dependent precursors of 24 nt siRNAs guiding de novo DNA methylation in Arabidopsis. *eLife* 4: e09591.
- Bologna NG, Voinnet O. 2014. The diversity, biogenesis, and activities of endogenous silencing small RNAs in Arabidopsis. *Annual Review of Plant Biology* 65: 473–503.
- Bouché N, Lauresergues D, Gascioli V, Vaucheret H. 2006. An antagonistic function for Arabidopsis DCL2 in development and a new function for DCL4 in generating viral siRNAs. *EMBO Journal* 25: 3347–3356.
- Brodersen P, Sakvarelidze-Achard L, Bruun-Rasmussen M, Dunoyer P, Yamamoto YY, Sieburth L, Voinnet O. 2008. Widespread translational inhibition by plant miRNAs and siRNAs. *Science* 320: 1185–1190.
- Bruenn JA. 1991. Relationships among the positive strand and double-strand RNA viruses as viewed through their RNA-dependent RNA polymerases. *Nucleic Acids Research* 19: 217–226.
- Bruenn JA. 2003. A structural and primary sequence comparison of the viral RNA-dependent RNA polymerases. *Nucleic Acids Research* 31: 1821–1829.
- Butterbach P, Verlaan MG, Dulleman A, Lohuis D, Visser RGF, Bai Y, Kormelink R. 2014. Tomato yellow leaf curl virus resistance by Ty-1 involves increased cytosine methylation of viral genomes and is compromised by cucumber mosaic virus infection. *Proceedings of the National Academy of Sciences, USA* 111: 12942–12947.
- Chen H, Kobayashi K, Miyao A, Hirochika H, Yamaoka N, Nishiguchi M. 2013. Both OsRecQ1 and OsRDR1 are required for the production of small RNA in response to DNA-damage in rice. *PLoS ONE* 8: e55252.
- Chitwood DH, Nogueira FTS, Howell MD, Montgomery TA, Carrington JC, Timmermans MCP. 2009. Pattern formation via small RNA mobility. *Genes & Development* 23: 549–554.
- Ciccarelli FD. 2006. Toward automatic reconstruction of a highly resolved tree of life. *Science* 311: 1283–1287.
- Cuerda-Gil D, Slotkin RK. 2016. Non-canonical RNA-directed DNA methylation. *Nature Plants* 2: 16163.
- Curaba J, Chen X. 2008. Biochemical activities of Arabidopsis RNA-dependent RNA polymerase 6. *Journal of Biological Chemistry* 283: 3059–3066.
- Dalmay T, Hamilton A, Rudd S, Angell S, Baulcombe DC. 2000. An RNA-dependent RNA polymerase gene in Arabidopsis is required for posttranscriptional gene silencing mediated by a transgene but not by a virus. *Cell* 101: 543–553.
- Das S, Swetha C, Pachamuthu K, Nair A, Shivaprasad PV. 2020. Loss of function of *Oryza sativa* Argonaute 18 induces male sterility and reduction in phased small RNAs. *Plant Reproduction* 33: 59–73.
- Devert A, Fabre N, Floris M, Canard B, Robaglia C, Crété P. 2015. Primer-dependent and primer-independent initiation of double stranded RNA synthesis by purified Arabidopsis RNA-dependent RNA polymerases RDR2 and RDR6. *PLoS ONE* 10: e0120100.
- Diaz-Pendon JA, Li F, Li W-X, Ding S-W. 2007. Suppression of antiviral silencing by cucumber mosaic virus 2b protein in Arabidopsis is associated with drastically reduced accumulation of three classes of viral small interfering RNAs. *Plant Cell* 19: 2053–2063.
- Duda CT. 1979. Synthesis of double-stranded RNA II. Partial purification and characterization of an RNA-dependent RNA polymerase in healthy tobacco leaves. *Virology* 92: 180–189.
- Fahlgrén N, Montgomery TA, Howell MD, Allen E, Dvorak SK, Alexander AL, Carrington JC. 2006. Regulation of AUXIN RESPONSE FACTOR3 by TAS3 ta-siRNA affects developmental timing and patterning in Arabidopsis. *Current Biology* 16: 939–944.
- Fei Q, Yang L, Liang W, Zhang D, Meyers BC. 2016. Dynamic changes of small RNAs in rice spikelet development reveal specialized reproductive phasiRNA pathways. *Journal of Experimental Botany* 67: 6037–6049.
- Fukunaga R, Doudna JA. 2009. dsRNA with 5' overhangs contributes to endogenous and antiviral RNA silencing pathways in plants. *EMBO Journal* 28: 545–555.
- Garcia D, Collier SA, Byrne ME, Martienssen RA. 2006. Specification of leaf polarity in Arabidopsis via the trans-acting siRNA pathway. *Current Biology* 16: 933–938.
- Gorbalenya AE, Pringle FM, Zeddiam JL, Luke BT, Cameron CE, Kalkmakoff J, Hanzlik TN, Gordon KHJ, Ward VK. 2002. The palm subdomain-based active site is internally permuted in viral RNA-dependent RNA polymerases of an ancient lineage. *Journal of Molecular Biology* 324: 47–62.
- Honda A, Mizumoto K, Ishihama A. 1986. RNA polymerase of influenza virus. Dinucleotide-primed initiation of transcription at specific positions on viral RNA. *Journal of Biological Chemistry* 261: 5987–5991.
- Hong W, Qian D, Sun R, Jiang L, Wang Y, Wei C, Zhang Z, Li Y. 2015. OsRDR6 plays role in host defense against double-stranded RNA virus, rice dwarf Phytoreovirus. *Scientific Reports* 5: 11324.
- Hsieh L-C, Lin S-I, Shih AC-C, Chen J-W, Lin W-Y, Tseng C-Y, Li W-H, Chiou T-J. 2009. Uncovering small RNA-mediated responses to phosphate deficiency in Arabidopsis by deep sequencing. *Plant Physiology* 151: 2120–2132.
- Hu B, Chu C. 2011. Phosphate starvation signaling in rice. *Plant Signaling & Behavior* 6: 927–929.
- Ikegami M, Fraenkel-Conrat H. 1979. Characterization of the RNA-dependent RNA polymerase of tobacco leaves. *Journal of Biological Chemistry* 254: 149–154.
- Jablonski SA, Morrow CD. 1995. Mutation of the aspartic acid residues of the GDD sequence motif of poliovirus RNA-dependent RNA polymerase results in enzymes with altered metal ion requirements for activity. *Journal of Virology* 69: 1532–1539.
- Jia Y, Lisch DR, Ohtsu K, Scanlon MJ, Nettleton D, Schnable PS. 2009. Loss of RNA-dependent RNA polymerase 2 (RDR2) function causes widespread and unexpected changes in the expression of transposons, genes, and 24-nt small RNAs. *PLoS Genetics* 5: e1000737.
- Johnson NR, Yeoh JM, Coruh C, Axtell MJ. 2016. Improved placement of multi-mapping small RNAs. *G3 Genes|Genomes|Genetics* 6: 2103–2111.
- Kao CC, Del Vecchio AM, Zhong W. 1999. De novo initiation of RNA synthesis by a recombinant flaviviridae RNA-dependent RNA polymerase. *Virology* 253: 1–7.
- Kapoor M, Arora R, Lama T, Nijhawan A, Khurana JP, Tyagi AK, Kapoor S. 2008. Genome-wide identification, organization and phylogenetic analysis of Dicer-like, Argonaute and RNA-dependent RNA polymerase gene families and their expression analysis during reproductive development and stress in rice. *BMC Genomics* 9: 451.
- Kawahara Y, de la Bastide M, Hamilton JP, Kanamori H, McCombie WR, Ouyang S, Schwartz DC, Tanaka T, Wu J, Zhou S *et al.* 2013. Improvement of the *Oryza sativa* Nipponbare reference genome using next generation sequence and optical map data. *Rice* 6: 4.
- Kim D, Pagei JM, Park C, Bennett C, Salzberg SL. 2019. Graph-based genome alignment and genotyping with HISAT2 and HISAT-genotype. *Nature Biotechnology* 37: 907–915.
- Kim J, Jung J-H, Reyes JL, Kim Y-S, Kim S-Y, Chung K-S, Kim JA, Lee M, Lee Y, Narry Kim V *et al.* 2005. microRNA-directed cleavage of ATHB15 mRNA regulates vascular development in Arabidopsis inflorescence stems. *The Plant Journal* 42: 84–94.
- Kim YG, Yoo JS, Kim JH, Kim CM, Oh JW. 2007. Biochemical characterization of a recombinant Japanese encephalitis virus RNA-dependent RNA polymerase. *BMC Molecular Biology* 8: 59.
- Komiya R, Ohyanagi H, Niihama M, Watanabe T, Nakano M, Kurata N, Nonomura K-I. 2014. Rice germline-specific Argonaute MEL1 protein binds to phasiRNAs generated from more than 700 lincRNAs. *The Plant Journal* 78: 385–397.
- Kumakura N, Takeda A, Fujioka Y, Motose H, Takano R, Watanabe Y. 2009. SGS3 and RDR6 interact and colocalize in cytoplasmic SGS3/RDR6-bodies. *FEBS Letters* 583: 1261–1266.
- Kumar S, Stecher G, Li M, Knyaz C, Tamura K. 2018. MEGA X: molecular evolutionary genetics analysis across computing platforms. *Molecular Biology and Evolution* 35: 1547–1549.



- Langmead B, Trapnell C, Pop M, Salzberg SL. 2009. Ultrafast and memory-efficient alignment of short DNA sequences to the human genome. *Genome Biology* 10: R25.
- Lee D-Y, An G. 2012. Two AP2 family genes, SUPERNUMERARY BRACT (SNB) and OsINDETERMINATE SPIKELET 1 (OsIDS1), synergistically control inflorescence architecture and floral meristem establishment in rice. *The Plant Journal* 69: 445–461.
- Lee WS, Fu SF, Li Z, Murphy AM, Dobson EA, Garland L, Chaluvadi SR, Lewsey MG, Nelson RS, Carr JP. 2016. Salicylic acid treatment and expression of an RNA-dependent RNA polymerase 1 transgene inhibit lethal symptoms and meristem invasion during tobacco mosaic virus infection in *Nicotiana benthamiana*. *BMC Plant Biology* 16: 15.
- Li Y, Li J, Chen Z, Wei Y, Qi Y, Wu C. 2020. OsmiR167a-targeted auxin response factors modulate tiller angle via fine-tuning auxin distribution in rice. *Plant Biotechnology Journal* 18: 2015–2026.
- Liu Y, Lee HC, Aalto AP, Yang Q, Chang SS, Huang G, Fisher D, Cha J, Poranen MM, Bamford DH. 2010. The DNA/RNA-dependent RNA polymerase QDE-1 generates aberrant RNA and dsRNA for RNAi in a process requiring replication protein A and a DNA helicase. *PLoS Biology* 8: e1000496.
- Lu C, Kulkarni K, Souret FF, MuthuVallippan R, Tej SS, Poethig RS, Henderson IR, Jacobsen SE, Wang W, Green PJ *et al.* 2006. MicroRNAs and other small RNAs enriched in the Arabidopsis RNA-dependent RNA polymerase-2 mutant. *Genome Research* 16: 1276–1288.
- Lu Y, Feng Z, Bian L, Xie H, Liang J. 2011. miR398 regulation in rice of the responses to abiotic and biotic stresses depends on CSD1 and CSD2 expression. *Functional Plant Biology* 38: 44.
- Makeyev EV, Bamford DH. 2002. Cellular RNA-dependent RNA polymerase involved in posttranscriptional gene silencing has two distinct activity modes. *Molecular Cell* 10: 1417–1427.
- Mallory AC, Reinhart BJ, Jones-Rhoades MW, Tang G, Zamore PD, Barton MK, Bartel DP. 2004. MicroRNA control of PHABULOSA in leaf development: importance of pairing to the microRNA 5' region. *EMBO Journal* 23: 3356–3364.
- Marin E, Jouannet V, Herz A, Lokerse AS, Weijers D, Vaucheret H, Nussbaum L, Crespi MD, Maizel A. 2010. miR390, Arabidopsis TAS3 tasiRNAs, and their AUXIN RESPONSE FACTOR targets define an autoregulatory network quantitatively regulating lateral root growth. *Plant Cell* 22: 1104–1117.
- Martin M. 2011. Cutadapt removes adapter sequences from high-throughput sequencing reads. *EMBnet journal* 17: 10.
- Matzke M, Kanno T, Daxinger L, Huettel B, Matzke AJM. 2009. RNA-mediated chromatin-based silencing in plants. *Current Opinion in Cell Biology* 21: 367–376.
- Matzke MA, Birchler JA. 2005. RNAi-mediated pathways in the nucleus. *Nature Reviews Genetics* 6: 24–35.
- Mourrain P, Béclin C, Elmayan T, Feuerbach F, Godon C, Morel J-B, Jouette D, Lacombe A-M, Nikic S, Picault N *et al.* 2000. Arabidopsis SGS2 and SGS3 genes are required for posttranscriptional gene silencing and natural virus resistance. *Cell* 101: 533–542.
- Nagasaki H, Itoh J-I, Hayashi K, Hibara K-I, Satoh-Nagasawa N, Nosaka M, Mukouhata M, Ashikari M, Kitano H, Matsuoka M *et al.* 2007. The small interfering RNA production pathway is required for shoot meristem initiation in rice. *Proceedings of the National Academy of Sciences, USA* 104: 14867–14871.
- Nishimura A, Ito M, Kamiya N, Sato Y, Matsuoka M. 2002. OsPNH1 regulates leaf development and maintenance of the shoot apical meristem in rice. *The Plant Journal* 30: 189–201.
- Nuthikattu S, McCue AD, Panda K, Fultz D, DeFraia C, Thomas EN, Keith SR. 2013. The initiation of epigenetic silencing of active transposable elements is triggered by RDR6 and 21–22 nucleotide small interfering RNAs. *Plant Physiology* 162: 116–131.
- Ogden KM, Ramanathan HN, Patton JT. 2012. Mutational analysis of residues involved in nucleotide and divalent cation stabilization in the rotavirus RNA-dependent RNA polymerase catalytic pocket. *Virology* 431: 12–20.
- Olmedo-Monfil V, Durán-Figueroa N, Arteaga-Vázquez M, Demesa-Arévalo E, Autran D, Grimanelli D, Slotkin RK, Martienssen RA, Vielle-Calzada J-P. 2010. Control of female gamete formation by a small RNA pathway in Arabidopsis. *Nature* 464: 628–632.
- Pachamuthu K, Swetha C, Basu D, Das S, Singh I, Sundar VH, Sujith TN, Shivaprasad PV. 2021. Rice-specific Argonaute 17 controls reproductive growth and yield-associated phenotypes. *Plant Molecular Biology* 105: 99–114.
- Pandey SP, Baldwin IT. 2007. RNA-directed RNA polymerase 1 (RdR1) mediates the resistance of *Nicotiana attenuata* to herbivore attack in nature. *The Plant Journal* 50: 40–53.
- Patel PH, Loeb LA. 2000. DNA polymerase active site is highly mutable: evolutionary consequences. *Proceedings of the National Academy of Sciences, USA* 97: 5095–5100.
- Paul AV, Van Boom JH, Filippov D, Wimmer E. 1998. Protein-primed RNA synthesis by purified poliovirus RNA polymerase. *Nature* 393: 280–284.
- Peragine A, Yoshikawa M, Wu G, Albrecht HL, Poethig RS. 2004. SGS3 and SGS2/SDE1/RDR6 are required for juvenile development and the production of trans-acting siRNAs in Arabidopsis. *Genes & Development* 18: 2368–2379.
- Polydore S, Axtell MJ. 2018. Analysis of RDR 1/RDR 2/RDR 6-independent small RNA s in *Arabidopsis thaliana* improves MIRNA annotations and reveals unexplained types of short interfering RNA loci. *The Plant Journal* 94: 1051–1063.
- Ranjith-Kumar CT, Gajewski J, Gutshall L, Maley D, Sarisky RT, Kao CC. 2001. Terminal nucleotidyl transferase activity of recombinant Flaviviridae RNA-dependent RNA polymerases: implication for viral RNA synthesis. *Journal of Virology* 75: 8615–8623.
- Sakai H, Lee SS, Tanaka T, Numa H, Kim J, Kawahara Y, Wakimoto H, Yang C-C, Iwamoto M, Abe T *et al.* 2013. Rice annotation project database (RAP-DB): an integrative and interactive database for rice genomics. *Plant and Cell Physiology* 54: e6.
- Schiebel W, Haas B, Marinkovic S, Klanner A, Sanger HL. 1993a. RNA-directed RNA polymerase from tomato leaves. I. Purification and physical properties. *Journal of Biological Chemistry* 268: 11851–11857.
- Schiebel W, Haas B, Marinkovic S, Klanner A, Sanger HL. 1993b. RNA-directed RNA polymerase from tomato leaves. I. Purification and physical properties. *Journal of Biological Chemistry* 268: 11851–11857.
- Schiebel W, Péliissier T, Riedel L, Thalmeir S, Schiebel R, Kempe D, Lottspeich F, Sanger HL, Wassenegger M. 1998. Isolation of an RNA-directed RNA polymerase-specific cDNA clone from tomato. *Plant Cell* 10: 2087–2101.
- Schwab R, Maizel A, Ruiz-Ferrer V, García D, Bayer M, Crespi M, Voinnet O, Martienssen RA. 2009. Endogenous TasiRNAs mediate non-cell autonomous effects on gene regulation in *Arabidopsis thaliana*. *PLoS ONE* 4: e5980.
- Schwab R, Ossowski S, Riester M, Warthmann N, Weigel D. 2006. Highly specific gene silencing by artificial microRNAs in Arabidopsis. *Plant Cell* 18: 1121–1133.
- Shivaprasad PV, Thillaichidambaram P, Balaji V, Veluthambi K. 2006. Expression of full-length and truncated Rep genes from Mungbean yellow mosaic virus-Vigna inhibits viral replication in transgenic tobacco. *Virus Genes* 33: 365–374.
- Singh J, Mishra V, Wang F, Huang H-Y, Pikaard CS. 2019. Reaction mechanisms of Pol IV, RDR2, and DCL3 drive RNA channeling in the siRNA-directed DNA methylation pathway. *Molecular Cell* 75: 576–589.e5.
- Song X, Wang D, Ma L, Chen Z, Li P, Cui X, Liu C, Cao S, Chu C, Tao Y *et al.* 2012. Rice RNA-dependent RNA polymerase 6 acts in small RNA biogenesis and spikelet development. *The Plant Journal* 71: 378–389.
- Sridevi G, Parameswari C, Sabapathi N, Raghupathy V, Veluthambi K. 2008. Combined expression of chitinase and  $\beta$ -1,3-glucanase genes in indica rice (*Oryza sativa* L.) enhances resistance against *Rhizoctonia solani*. *Plant Science* 175: 283–290.
- Stocks MB, Moxon S, Mapleson D, Woolfenden HC, Mohorianu I, Folkes L, Schwach F, Dalmay T, Moulton V. 2012. The UEA sRNA workbench: a suite of tools for analysing and visualizing next generation sequencing microRNA and small RNA datasets. *Bioinformatics* 28: 2059–2061.
- Sun W, Xu XH, Li Y, Xie L, He Y, Li W, Lu X, Sun H, Xie X. 2020. OsmiR530 acts downstream of OsPIL15 to regulate grain yield in rice. *New Phytologist* 226: 823–837.
- Sunkar R, Kapoor A, Zhu JK. 2006. Correction. *Plant Cell* 18: 2415.
- Tang G. 2003. A biochemical framework for RNA silencing in plants. *Genes & Development* 17: 49–63.
- Trapnell C, Williams BA, Pertea G, Mortazavi A, Kwan G, van Baren MJ, Salzberg SL, Wold BJ, Pachter L. 2011. Transcript assembly and abundance



- estimation from RNA-Seq reveals thousands of new transcripts and switching among isoforms. *Nature Biotechnology* 28: 511–515.
- Vaucheret H. 2008. Plant ARGONAUTS. *Trends in Plant Science* 13: 350–358.
- Vazquez F, Vaucheret H, Rajagopalan R, Lepers C, Gascioli V, Mallory AC, Hilbert JL, Bartel DP, Cr     P. 2004. Endogenous trans-acting siRNAs regulate the accumulation of Arabidopsis mRNAs. *Molecular Cell* 16: 69–79.
- Verlaan MG, Hutton SF, Ibrahim RM, Kormelink R, Visser RGF, Scott JW, Edwards JD, Bai Y. 2013. The tomato yellow leaf curl virus resistance genes Ty-1 and Ty-3 are allelic and code for DFDGD-class RNA-dependent RNA polymerases. *PLoS Genetics* 9: e1003399.
- Voinnet O. 2008. Use, tolerance and avoidance of amplified RNA silencing by plants. *Trends in Plant Science* 13: 317–328.
- Wang J, Bao J, Zhou B, Li M, Li X, Jin J. 2021. The osa-miR164 target OsCUC1 functions redundantly with OsCUC3 in controlling rice meristem/organ boundary specification. *New Phytologist* 229: 1566–1581.
- Wang N, Zhang D, Wang Z, Xun H, Ma J, Wang H, Huang W, Liu Y, Lin X, Li N *et al.* 2014. Mutation of the RDR1 gene caused genome-wide changes in gene expression, regional variation in small RNA clusters and localized alteration in DNA methylation in rice. *BMC Plant Biology* 14: 177.
- Wang XB, Wu Q, Ito T, Cillo F, Li WX, Chen X, Yu JL, Ding SW. 2010. RNAi-mediated viral immunity requires amplification of virus-derived siRNAs in *Arabidopsis thaliana*. *Proceedings of the National Academy of Sciences, USA* 107: 484–489.
- Warthmann N, Chen H, Ossowski S, Weigel D, Herv   P. 2008. Highly specific gene silencing by artificial miRNAs in rice. *PLoS ONE* 3: e1829.
- Wassenegger M, Krczal G. 2006. Nomenclature and functions of RNA-directed RNA polymerases. *Trends in Plant Science* 11: 142–151.
- Williams L, Carles CC, Osmont KS, Fletcher JC. 2005. A database analysis method identifies an endogenous trans-acting short-interfering RNA that targets the Arabidopsis ARF2, ARF3, and ARF4 genes. *Proceedings of the National Academy of Sciences, USA* 102: 9703–9708.
- Willmann MR, Endres MW, Cook RT, Gregory BD. 2011. The functions of RNA-dependent RNA polymerases in Arabidopsis. *The Arabidopsis Book* 9: e0146.
- Wu L, Zhang Q, Zhou H, Ni F, Wu X, Qi Y. 2009. Rice microRNA effector complexes and targets. *Plant Cell* 21: 3421–3435.
- Wu L, Zhou H, Zhang Q, Zhang J, Ni F, Liu C, Qi Y. 2010. DNA methylation mediated by a microRNA pathway. *Molecular Cell* 38: 465–475.
- Xie Z, Fan B, Chen C, Chen Z. 2001. An important role of an inducible RNA-dependent RNA polymerase in plant antiviral defense. *Proceedings of the National Academy of Sciences, USA* 98: 6516–6521.
- Xie Z, Johansen LK, Gustafson AM, Kasschau KD, Lellis AD, Zilberman D, Jacobsen SE, Carrington JC. 2004. Genetic and functional diversification of small RNA pathways in plants. *PLoS Biology* 2: e104.
- Yang SJ, Carter SA, Cole AB, Cheng NH, Nelson RS. 2004. A natural variant of a host RNA-dependent RNA polymerase is associated with increased susceptibility to viruses by *Nicotiana benthamiana*. *Proceedings of the National Academy of Sciences, USA* 101: 6297–6302.
- Yoshikawa M. 2005. A pathway for the biogenesis of trans-acting siRNAs in Arabidopsis. *Genes & Development* 19: 2164–2175.
- Zhang DX, Spiering MJ, Nuss DL. 2014. Characterizing the roles of *Cryphonectria parasitica* RNA-dependent RNA polymerase-like genes in antiviral defense, viral recombination and transposon transcript accumulation. *PLoS ONE* 9: e108653.
- Zhang J-P, Yu Y, Feng Y-Z, Zhou Y-F, Zhang F, Yang Y-W, Lei M-Q, Zhang Y-C, Chen Y-Q. 2017. MiR408 regulates grain yield and photosynthesis via a phytoecyanin protein. *Plant Physiology* 175: 1175–1185.
- Zhang T, Li Y, Ma L, Sang X, Ling Y, Wang Y, Yu P, Zhuang H, Huang J, Wang N *et al.* 2017. LATERAL FLORET 1 induced the three-florets spikelet in rice. *Proceedings of the National Academy of Sciences, USA* 114: 9984–9989.
- Zhao Y, Peng T, Sun H, Teotia S, Wen H, Du Y, Zhang J, Li J, Tang G, Xue H *et al.* 2019. miR1432- Os ACOT (Acyl-CoA thioesterase) module determines grain yield via enhancing grain filling rate in rice. *Plant Biotechnology Journal* 17: 712–723.

## Supporting Information

Additional Supporting Information may be found online in the Supporting Information section at the end of the article.

**Dataset S1** Differentially expressed genes in RDR3 OE transgenic lines.

**Dataset S2** Differentially expressed genes in RDR3 KD transgenic lines.

**Dataset S3** Differentially expressed sRNA loci in RDR3 OE and KD plants compared with WT.

**Fig. S1** Expression analysis of  $\gamma$ -clade RDRs, OsRDR3 and OsRDR4.

**Fig. S2** Generation of OsRDR3 OE and amiR lines and their regeneration response.

**Fig. S3** Molecular analysis of OsRDR3 OE and KD transgenic lines.

**Fig. S4** Generation of transgenic *Nicotiana tabacum* plants overexpressing OsRDR3.

**Fig. S5** Molecular analysis of OsRDR4 OE transgenic lines.

**Fig. S6** Molecular analysis of OsRDR4 amiR transgenic lines.

**Fig. S7** Abundance distribution of sRNAs mapping to different genomic regions in OsRDR3 transgenic plants.

**Fig. S8** Percentage distribution of sRNAs mapping to different genomic regions in OsRDR4 transgenic plants.

**Fig. S9** Effect of RNA silencing mutants on OsRDR3 loci.

**Fig. S10** Genome browser pictures of repeat loci showing differential change across WT and OsRDR3 transgenic plants.

**Fig. S11** Genome browser pictures of genomic regions showing differential change across WT and OsRDR3 transgenic plants.

**Fig. S12** Genome browser pictures of genomic regions showing differential change across WT and OsRDR3 transgenic plants.

**Fig. S13** Genome browser pictures of genomic regions showing differential change across WT and OsRDR3 transgenic plants.

**Fig. S14** Isolation, molecular verification and polymerase activity of MBP : RDR3 fusion protein.

**Fig. S15** Immunoprecipitation of OsRDR3 WT, its catalytic domain mutant and its polymerase activity.

**Fig. S16** Uncropped images of the main Figs 7 and 8.

**Fig. S17** Uncropped images of the Figs S14 and 15.

**Method S1** RT-qPCR.

**Method S2** Southern blotting.

**Method S3** Semiquantitative RT-PCR.

**Method S4** sRNA northern analysis.

**Method S5** Immunoprecipitation of GFP-RDR3 with GFP-trap.

**Method S6** Purification of GFP-Nanobody.

**Method S7** Immunoprecipitation of GFP-RDR3 with GFP-Nanobody.

**Table S1** DNA and RNA oligos used in the study.

**Table S2** miRNA abundance in WT, OsRDR3 OE and KD transgenic rice plants.

**Table S3** Details of library statistics used in sRNA and RNA-seq datasets.

**Table S4** Abundance of 21-nt siRNAs in 21-nt phased sRNA loci between WT, RDR3 OE and KD lines.

**Table S5** Abundance of 24-nt siRNAs in 24nt phased sRNA loci between WT, RDR3 OE and KD lines.

Please note: Wiley Blackwell are not responsible for the content or functionality of any Supporting Information supplied by the authors. Any queries (other than missing material) should be directed to the *New Phytologist* Central Office.